Spring 2018

Driving Sortase-Mediated Ligations Using Metal-Coordinating Peptides

Sierra Reed
Western Washington University, sierrambereed@gmail.com

Driving Sortase-Mediated Ligations Using Metal-Coordinating Peptides

By

Sierra Reed

Accepted in Partial Completion
of the Requirements for the Degree
Master of Science

ADVISORY COMMITTEE

Chair, Dr. John Antos

Dr. Spencer Anthony-Cahill

Dr. P. Clint Spiegel

GRADUATE SCHOOL

Dr. Gautam Pillay, Dean

Master's Thesis

In presenting this thesis in partial fulfillment of the requirements for a master's degree at Western Washington University, I grant to Western Washington University the non-exclusive royalty-free right to archive, reproduce, distribute, and display the thesis in any and all forms, including electronic format, via any digital library mechanisms maintained by WWU.

I represent and warrant this is my original work and does not infringe or violate any rights of others. I warrant that I have obtained written permissions from the owner of any third party copyrighted material included in these files.

I acknowledge that I retain ownership rights to the copyright of this work, including but not limited to the right to use all or part of this work in future works, such as articles or books.

Library users are granted permission for individual, research and non-commercial reproduction of this work for educational purposes only. Any further digital posting of this document requires specific permission from the author.

Any copying or publication of this thesis for commercial purposes, or for financial gain, is not allowed without my written permission.

Sierra Reed
5/29/2018

Driving Sortase-Mediated Ligations Using Metal-Coordinating Peptides

A Thesis Presented to
The Faculty of Western Washington University

In Partial Fulfillment of the
Requirements for the Degree
Master of Science

by
Sierra Reed
May 2018

Abstract

The versatility of sortase-mediated ligations as a protein modification technique has been well demonstrated, but the efficiency of these reactions suffers from inherent reversibility. Solutions to this issue have been reported, however these methods are accompanied by additional limitations of the sortase-mediated ligation (SML) strategy. A preferable methodology would include the smallest possible modification site without restricting the point of ligation. One promising solution to this issue is the expansion of the LPXTG SrtA recognition sequence to LPXTGGH, giving the excised fragment an N-terminal GGH motif. This minor alteration has been shown to allow complexation of the excised fragment with Ni^{2+} ions, thus sequestering this component from the reaction and improving yields through hindered reversibility. In this thesis, we explore the scope of this metal-assisted sortase-mediated ligation (MASML) approach, including the Ni^{2+}-enhanced modification of full sized proteins with a number of useful chromophores. Furthermore, this approach was shown to be compatible with the installation of PEG and a cyclooctyne bioorthogonal ligation handle. In total, this work demonstrates that MASML is compatible with a range of high value protein targets and modifications, and shows how MASML is a straightforward method for improving the efficiency of sortase-mediated protein engineering strategies.

Acknowledgements

I owe a great deal of thanks to Dr. John Antos for his guidance throughout the course of this project, as well as the initial opportunity to partake in undergraduate research in his lab. My experience here has helped to build my passion for research and greatly influenced where I plan to go with my career in the future. He has also been a great presence in lab and his enthusiasm for the work we do has truly inspired my own.

I would also like to thank the previous and current member of the Antos lab, especially Orion Banks, David Brzovic, Natasha Hessami, Nicholas Horvath, and Sarah Bowersox. David's initial work and guidance on this nickel project was imperative to the success of my own, and Orion's constant patience and tutelage in lab techniques has been endlessly appreciated. Nick, Natasha, and Sarah have been wonderful sources of feedback in both my research and academic careers.

In addition, I am grateful to the other members of my committee, Dr. P. Clint Spiegel and Dr. Spencer Anthony-Cahill, for their feedback over the course of writing this thesis. I also thank Western Washington University and the National Institutes of Health for funding this project (Grant: 1RI5GMII9048-01).

Finally, I would like to give special thanks to Ardi Kveven and the staff of ORCA for being a constant source of inspiration and undeniable contributors to my successes, both academic and personal.

Table of Contents

List of Figures and Tables

List of Abbreviations and Acronyms

6-FAM	6-carboxyfluoroscein
ADC	Antibody-drug conjugate
Boc	*tert*-Butyloxycarbonyl
Cy3	Cyanine3
DARPin	Design ankyrin repeat protein
DBCO	Dibenzocyclooctyne
DCM	Dichloromethane
DEAC	7-(diethylamino)coumarin-3-carboxylic acid
DIPEA	Diisopropylethylamine
DMSO	Dimethylsulfoxide
EDTA	Ethylenediaminetetraacetic acid
ESI-MS	Electrospray ionization mass spectrometry
Fmoc	Fluorenylmethyloxycarbonyl
FPLC	Fast protein liquid chromatography
HPLC	High performance liquid chromatography
IMAC	Immobilized metal affinity chromatography
IPTG	Isopropyl-β-D-1-thiogalactopyranoside
MASML	Metal-assisted sortase-mediated ligation
MBHA	4-methylbenzhydrylamine
MeCN	Acetonitrile
Ni-NTA	Nickel nitriloacetic acid
NHS	N-hydoxysuccinimide

NMP	N-methyl-2-pyrrolidinone
OD_{600}	Optical density at 600nm
PAGE	Polyacrylamide gel electrophoresis
PEG	Polyethylene glycol
sAff	Affibody protein containing SrtA recognition sequence
sDARP	DARPIN protein containing SrtA recognition sequence
SDS	Sodium dodecyl sulfate
sFh8	Fh8 solubility tag containing SrtA recognition sequence
sFyn	Fynomer protein containing SrtA recognition sequence
SML	Sortase-mediated ligation
sMon	Monobody protein containing SrtA recognition sequence
SPPS	Solid-phase peptide synthesis
$SrtA_{5mut}$	Penta-mutant of the Sortase A enzyme from *Staphylococcus aureus*
$SrtA_{7mut}$	Hepta-mutant of the Sortase A enzyme from *Staphylococcus aureus*
$SrtA_{Staph}$	*Staphylococcus aureus* Sortase A
TFA	Trifluoroacetic acid
TFP	Tetrafluorophenol
Tris	Tris(hydroxymethyl)aminomethane
UV/Vis	Ultraviolet/visible spectroscopy

1. Introduction

1.1 Overview of Protein Engineering Techniques

The use of protein engineering to generate molecules with novel functionality is an ever-growing field of research, with academic, industrial, and medical applications. Techniques vary, with the most basic being molecular biology techniques to modify proteins on a genetic level. Simple point mutations, sequence deletions and additions[1] are all useful for investigating protein structure and function, but the dependence on rational design as well as typically being restricted to naturally occurring amino acids, imposes a limitation on the type of alterations one can make to protein structures. Great strides have been made to circumvent these limitations, notably in the areas of directed evolution[2–4] and unnatural amino acid mutagenesis[5–8]. However, these techniques remain time consuming and expensive, and thus there continues to be a need for complementary protein engineering techniques.

In contrast to genetic approaches, direct chemical modification of proteins provides a quick and experimentally facile way to access altered protein structures. By taking advantage of the natural chemistry of amino acid side chains such as cysteine, lysine, glutamic and aspartic acids, one can append non-natural modifications to an already properly folded protein structure. This has been used for chromophore-[9] and radio-labeling,[10] the attachment of drugs in the context of therapeutics,[11] and the introduction of structures to improve half-life and solubility *in vivo*.[12,13] For example, the modification of lysine residues is one of the most widely used forms of chemical-based protein modification, performed by introducing reagents consisting of a desired modification, tethered to an amine-reactive functional group such as an N-hydroxysuccinimidal ester.

Lysine side chains are able to act as nucleophiles, resulting in the covalent attachment of the desired functional group. Reagents for the selective modification of cysteine, aspartic and glutamic acid, and a range of other amino acids are also readily available.[14] However, these reactions generally lack site-selectivity. While the reagents used can differentiate between the types of side-chains, it is difficult to distinguish between copies of the same residue. Therefore, these techniques typically lead to polydisperse, non-specific modifications. While this heterogeneity may be permissible for applications such as fluorescent protein labeling, it may be incompatible with more demanding applications such as the production of defined protein-drug conjugates.

More recently, chemoenzymatic approaches have emerged that combine the most desirable attributes of genetic and chemical methods for protein engineering.[15] Chemoenzymatic strategies take advantage of the pre-existing protein modification activity of enzymes, which have evolved to recognize specific amino-acid sequences within their complementary substrates (**Figure 1**). When these substrates are incorporated into protein targets of interest, the corresponding enzyme can then be used to site-specifically install useful modifications. By enabling a wide range of useful transformations on an even wider range of targets, enzymes provide a library of natural tools for modification chemistry. Chemoenzymatic techniques therefore provide advantages over traditional protein engineering approaches, specifically in the ability to generate consistent, monodisperse constructs, by virtue of the genetically encoded recognition sequence.

These methods also allow for considerable flexibility in the types of modifications installed, as many enzymes used in chemoenzymatic approaches can utilize diverse

synthetic small molecule reagents, so long as they contain the appropriate molecular features required for recognition by the enzyme. Advances in screening techniques have also lead to the directed evolution of enzymes with a broadened scope of targets and allowable modifications.[16,17] Enzymatic processes can also be manipulated *in vitro* to allow for the site-specific installation of short peptides or synthetic chemical modifications such as chromophores,[18–22] click handles,[23–26] or pharmaceuticals.[27]

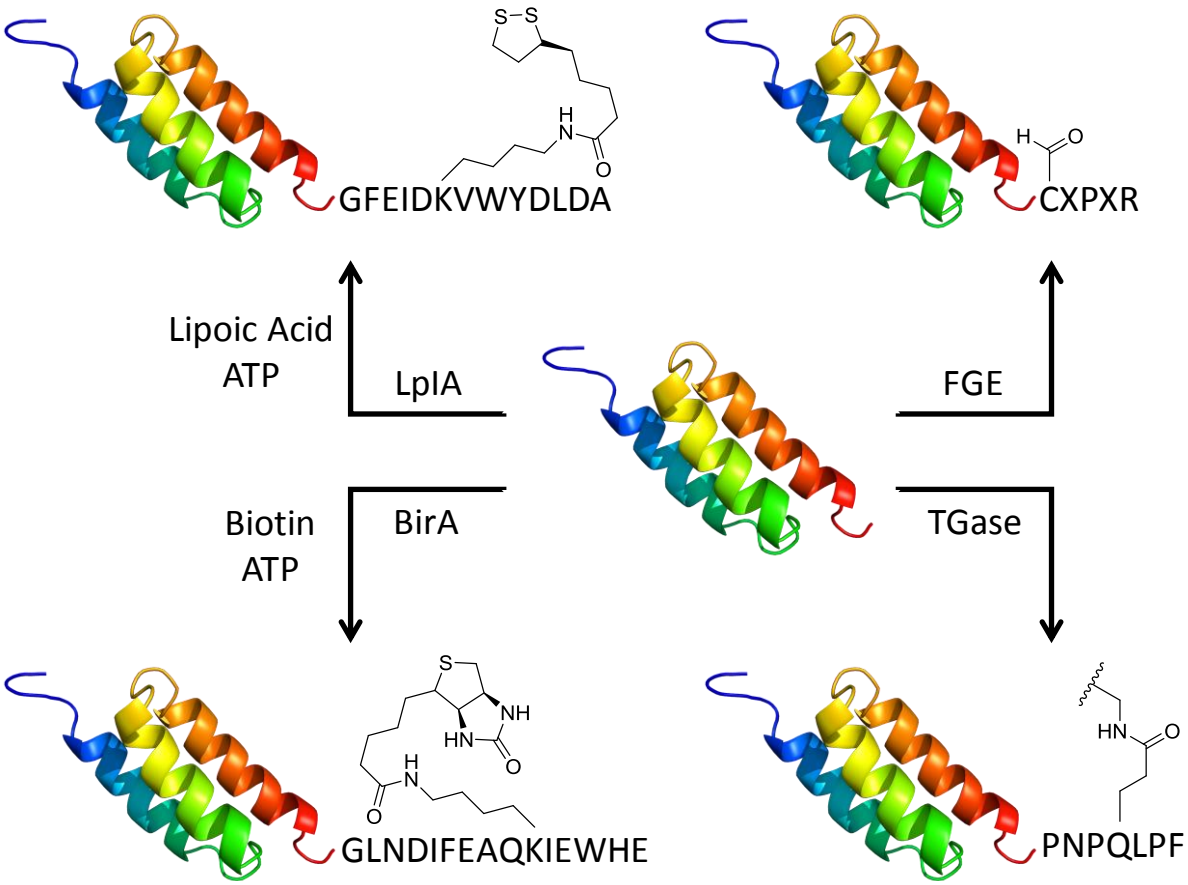

Figure 1. Representative chemoenzymatic approaches for protein modification.

Examples of enzymes used for chemoenzymatic protein labeling include formyl glycine generating enzyme,[28] which converts cysteine residues to aldehydes for further bioconjugation with aminooxy and hydrazide reagents; transglutaminase,[29] used for the crosslinking of glutamine with lysine sidechains or other free amines; biotin[30] and lipoic

acid ligases,[31] which append their respective modifications to lysine sidechains through the hydrolysis of ATP; and the bacterial sortases,[32–36] transpeptidases which cleave their target sequence and append modifications to the protein termini.

1.2 Adapting Sortase A for Chemoenzymatic Protein Labeling

First characterized by Schneewind and colleagues in 1999,[35] sortase enzymes were discovered in the cell walls of most gram-positive bacteria, and to date six classes (A-E) of these enzymes gave been described.[33] Class A (SrtA), the most thoroughly characterized of the sortase family, consists of 'housekeeping' enzymes which aide in the incorporation of numerous proteins, including virulence factors, into the bacterial cell wall.[35] Class B attach heme-receptors to peptidoglycans,[37] and participate in the construction of bacterial pili.[38] Class C are also involved in pilus formation and are noteworthy for their ability to form isopeptide bonds.[39,40] Class D is found predominantly in *Bacilli* and has been implicated in the anchoring of cell wall proteins which allow for bacterial sporulation.[41] Comparatively little is known about classes E and F, though the class F sortase found in *Corynebacterium diptheriae* has been shown to perform housekeeping functions similar to SrtA.[42]

Sortases, while interesting in their importance to the virulence of pathogenic bacteria, have also proven useful as tools for protein modification.[23,43] *In vivo*, SrtA from *S. aureus* ($SrtA_{Staph}$) specifically has been frequently used as a chemoenzymatic approach for protein modification, and sortase-mediated ligation (SML) is now a widely used technique. SrtA acts by recognizing an LPXTG motif (where X can be any amino acid) and cleaving between the threonine and glycine residues (**Figure 2**). This is

achieved through nucleophilic attack of the amide bond by a highly conserved active-site cysteine. The glycine and remainder of the target molecule's C-terminus becomes what will heretofore be termed the "excised fragment", while the N-terminal portion of the substrate remains covalently linked to the sortase enzyme. The resulting thioester bond is then itself susceptible to nucleophilic attack by an N-terminal glycine residue, yielding the final ligation product. The sorting-sequence containing molecule is often a nascent virulence factor, while the nucleophile is the pentaglycine head of lipid II, a cell wall precursor. However, this reaction can also be performed *in vitro* with a variety of ligation partners, including live cells,[19–21] solid supports,[44] full sized proteins,[18,23–25,27,44] chromophores[18,20–22,45] and other small molecule modifications[46] (**Figure 3**). It should be noted, recombinant $SrtA_{Staph}$ requires Ca^{2+} for optimal activity *in vitro*.

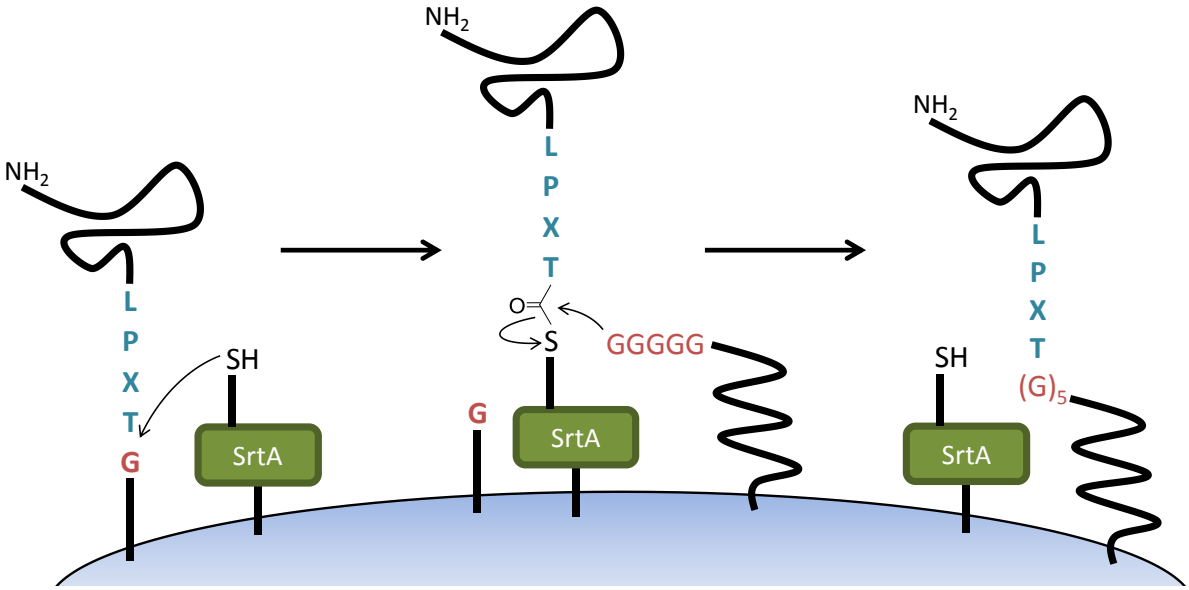

Figure 2. Sortase A-mediated cell wall anchoring *in vivo*.

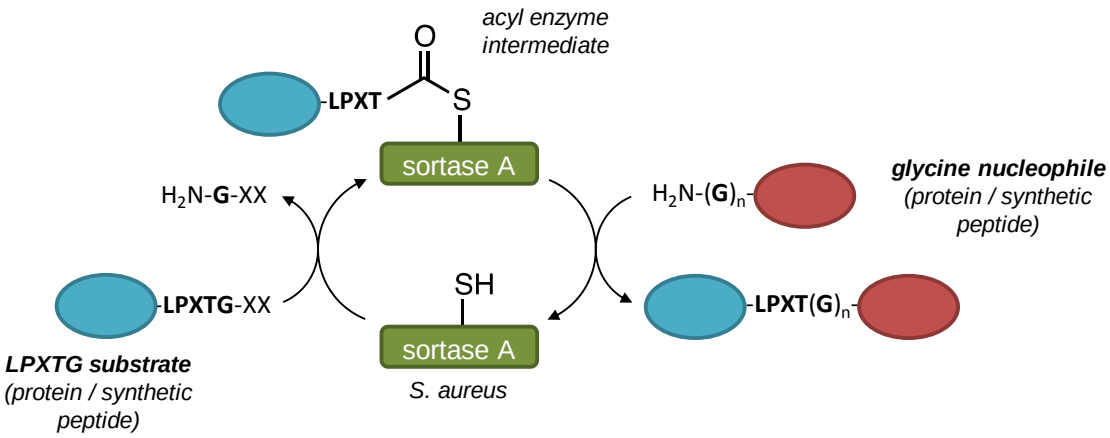

Figure 3. General ligation mechanism of sortase A.

Example applications of SML include the generation of antibody drug conjugates (ADCs), as was shown by Beerli *et al*. in 2015.[27] Their group demonstrated how SML-generated equivalents of commercial ADCs such as the anti-CD30 brentuximab vedotin (Adcetris) and anti-HER-2 trastuzumab emtansine (Kadcyla) performed identically to the traditional constructs during *in vitro* assays. The sortase-generated trastuzumab-maytansine was also shown to have similar activity to Kadcyla in mice models. Another study by the Park group examined the use of SML for the direct labeling of live cells by introducing sortase-ready fluorescent markers (EGFP-LPETG$_5$ and TAMRA-LPETG$_5$) to HeLa cells expressing SrtA on their surface.[20] These cells were shown to fluoresce, due to the formation of a conjugate between the fluorescent substrates and the sortase molecules, while controls treated with non-compatible substrates (EGFP-LPETA$_5$ and TAMRA-LPATA$_5$) did not form the conjugate, and therefore did not exhibit fluorescence. In addition to applications for direct conjugation chemistry, SML can also be used to introduce secondary conjugation sites for additional biorthogonal modifications, such as the incorporation of click handles. Krueger *et al.* demonstrated the benefits of this method

by using SML to introduce tetrazine- and alkene-baring linkers of varying lengths to protein ligands which were further conjugated together via a bioorthogonal click reaction.[25] This provided a simplified method of testing variable linker lengths, as it allowed for the use of the same sortase-ready protein substrates, with alterations only being required of the small synthetic linkers. In total, these studies exemplify some of the common uses of SML as a protein modification technique.

The sortase enzyme itself has also been modified to better suit *in vitro* applications. As indicated above, a commonly used and well characterized form is the SrtA homolog from *Staphylococcus aureus,* $SrtA_{Staph}$. The enzyme is typically used in a truncated mutant form (Δ59), lacking the first 59 amino acid residues, which correspond to the transmembrane domain which would anchor sortase *in vivo*. This truncation allows for $SrtA_{Staph}$ to be expressed in soluble form and used effectively in aqueous solutions (**Figure 3**). A further mutant, designed to not possess a typical N-terminal glycine, is also used to prevent non-target interaction of the acyl-enzyme intermediate with a second sortase enzyme acting as a nucleophile.

Further modification was performed to the enzyme in 2011 through directed evolution using yeast display to select for mutations which increased reaction kinetics through improved substrate binding.[47] The end result was a penta-mutant $SrtA_{Staph}$ ($SrtA_{5mut}$) with improved binding affinity for both LPXTG and N-terminal glycine substrates, and a 120-fold increase in k_{cat}/K_M. In 2012, another study showed how Ca^{2+}-independence could be achieved through the mutation of two glutamates within the calcium-binding pocket of $SrtA_{Staph}$.[48] However, these mutations proved to be detrimental to the overall activity of the enzyme, which showed a more than 3-fold decrease in k_{cat}.

Hirakawa *et al*., who originally demonstrated these effects, later combined these two mutations with those of the penta-mutant, in the hopes of improving kinetics while maintaining Ca^{2+} independence. The resulting hepta-mutant ($SrtA_{7mut}$) exhibited an 8-fold increase in $k_{cat}/K_{M\ LPETG}$ and a 4-fold increase in $k_{cat}/K_{M\ GGG}$.[48] Both the penta- and hepta-mutants provide improvements to the typical SML reaction and have been used to perform faster and more efficient ligations than achievable with wild-type $SrtA_{Staph}$.

1.3 Current Techniques for Limiting Reversibility of the Sortase Reaction

While a widely used ligation technique, like most enzymatic methodologies sortase has its limitations. In the case of SML, the inherent reversibility of the reaction is a frequently cited drawback.[43] As mentioned previously sortase acts by first recognizing an LPXTG motif in its target substrate, but this sequence is also present in the final ligation product. This allows the product to be recognized by the sortase enzyme, and in turn causes cleavage of the desired modification and replacement by the initial excised fragment. Overall, this results in regeneration of starting substrate protein and the initial glycine nucleophile. For this reason, most sortase-mediated ligations performed with equimolar concentrations of substrate and nucleophile typically reach only 50% completion.

To improve ligation efficiency, a growing number of solutions have been described. The most straightforward of these is to include an excess of one of the ligation partners. This drives the reaction equilibrium towards products and increases yields accordingly, however this is not ideal if the reagents being used in excess are either costly, difficult to prepare, or difficult to remove from the final reaction mixture.

More modern methods for controlling the reaction equilibrium have focused on deactivating certain products of the SML reaction, preventing them from re-entering the catalytic cycle. The first of these methods for enhancing ligation efficiency was introduced by Yamamura and colleagues and involves inducing the formation of a β-hairpin upon ligation (**Figure 4**).[49] This is achieved by incorporating Trp-Thr repeats upstream of the sorting sequence of the substrate and downstream of the nucleophile's N-terminus. Upon ligation a 'Trp zipper' is formed, effectively hindering interaction of the reformed LPXTG motif with the SrtA active site. Using equimolar concentrations of the starting materials, yields were improved from 50% to ~70%, over the course of a 24hr reaction. The ligation products were also shown to have long-lasting resistance to SrtA cleavage, even in the presence of excess triglycine nucleophile. While effective at improving yields, the introduction of secondary structure around the ligation site, and the expansion of the ligation site itself, is not ideal, as one begins to risk interference with the folding and function of the desired protein ligation product.

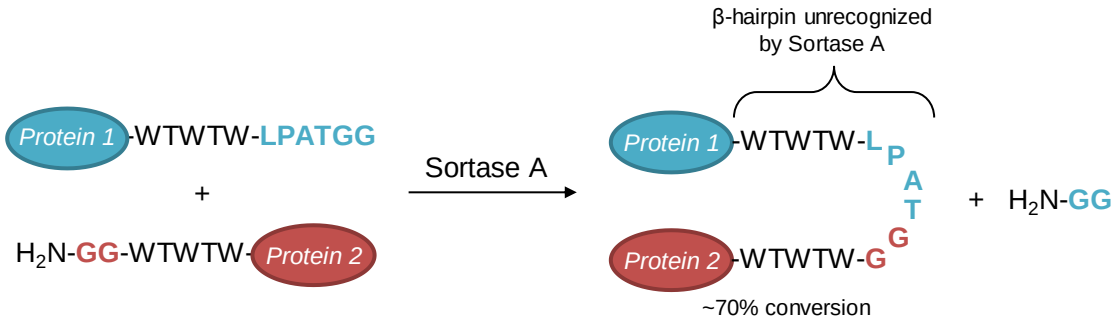

Figure 4. Ligation product deactivation technique described by Yamamura *et al*. for the improvement of SML yields.[49]

In addition to β-hairpins, other techniques take advantage of deactivated excised fragment molecules, specifically by reducing the nucleophilicity of these species. Williamson *et al*. achieved this by generating synthetic depsipeptide substrates containing an unnatural diglycine mimic within the LPXTG sequence (**Figure 5a**).[43] The substrate, which has an ester in place of the native Thr-Gly amide bond, produces an N-terminal hydroxyl group upon cleavage. This is a considerably weaker nucleophile compared to the amine of an N-terminal glycine and prevents the alcohol by-product from participating in a reverse ligation reaction. Similarly, Liu *et al*. showed that by incorporating isoacyl-Ser or isoacyl-Hse two residues downstream of the recognition sequence, a spontaneous diketopiperanzine formation deactivates the excised fragment, thus favoring product formation (**Figure 5b**).[50] Both strategies require the substrates to be produced through solid-phase peptide synthesis, thus limiting modifications to the N-terminus of protein targets.

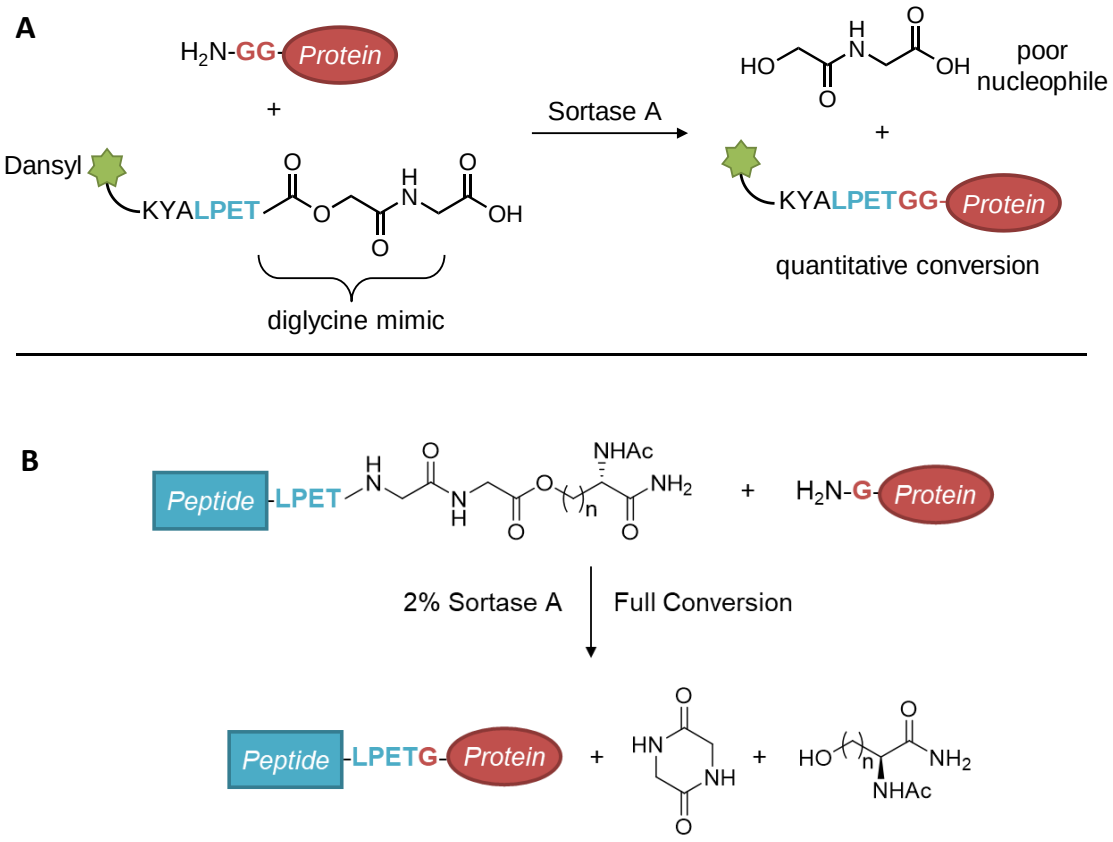

Figure 5. Nucleophile deactivation techniques proposed by Williamson *et al*.[43] **(A)** and Liu *et al*.[50] **(B)** for the improvement of SML yields.

Given the limitations of the previous strategies for boosting SML efficiency, we sought to develop a new approach which would ideally (1) maintain the minimal size of the SML ligation site (LPXTG), (2) be applicable to a broad range of SML applications involving modification of the protein N- or C-terminus, and (3) not require significant synthetic modification of the peptide modifying agents generally used for SML. Additionally, the technique should allow for high ligation yields in idealized, equimolar substrate conditions, to make the reaction as cost effective and efficient as possible.

A strategy meeting these criteria was introduced by Row *et al*., who proposed that by the simple expansion of the sortase recognition sequence to LPXTGGH, the excised fragment would be capable of coordinating with Ni^{2+} via the new N-terminal GGH motif

(**Figure 6**).[51] The metal-peptide complex, anchored through the histidine residue, was shown to effectively sequester the nucleophilic lone pair of the N-terminal glycine, reducing the overall nucleophilicity of the excised fragment.

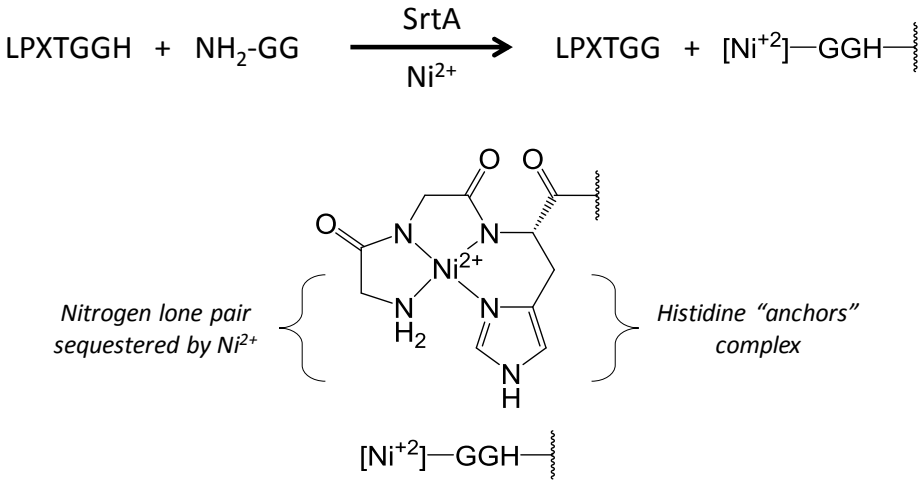

Figure 6. Structure of the complex formed between Ni^{2+} and the N-terminus of the GGH excised fragment.

In contrast to previous methodologies for improving SML efficiency, this approach to deactivating one of the ligation products does not require changes to the size of the final sortase ligation site or the use of complex synthetic substrate mimetics. Moreover, the expanded recognition sequence includes no non-natural amino acids and can therefore be synthesized by standard solid phase peptide synthesis (SPPS) or encoded into protein targets at the genetic level. In the initial report, this technique was demonstrated most thoroughly in the context of small peptide substrates and nucleophiles, with ligation yields improved from 60% to over 80% when working at equimolar concentrations (**Figure 7**).[51] While effective with peptides, the application of this metal-assisted sortase-mediated ligation (MASML) approach to larger protein targets

was minimal and involved only two examples focused on the C-terminal modification of maltose binding protein and the N-terminal modification of insulin.

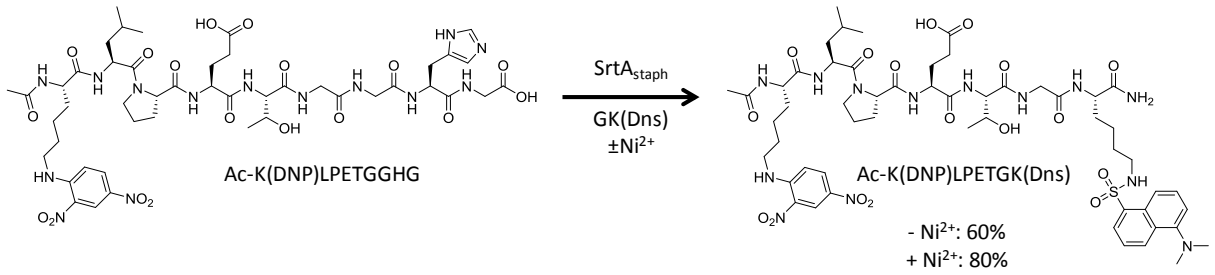

Figure 7. Example MASML reaction performed on small molecule reagents by Row *et al*.[51]

1.4 Project Goals and Overview

The applicability of metal-assisted sortase-mediated ligation (MASML) to the modification of full-sized proteins has not been as thoroughly studied as small peptide applications. Given the prevalent use of sortase as a protein modification tool, it was therefore made the goal of this project to demonstrate a fuller scope of protein applications for MASML, using a variety of protein targets in conjunction with a range of industrially and medically relevant protein modifying agents.

To this end, this thesis describes the expression and purification of multiple small protein targets which represent alternative, non-antibody scaffolds for molecular recognition. These proteins were prepared with a MASML-expanded SrtA recognition sequence (LPETGGH), with the histidine being the first residue of a standard C-terminal His_6 affinity tag. Notably, this sequence is common in sortase-ready protein substrates which have been reported in the literature.[18,19,22,23,26,44,46,52] A suite of small peptide nucleophiles was also generated, equipped with a range of protein modifiers including fluorophores, PEG, and a bioorthogonal reaction handle. With these materials, we have succeeded in demonstrating how MASML is compatible with numerous model protein

modification reactions, resulting in significant improvements in ligation efficiency when reactions were conducted in the presence of Ni^{2+} ions. In addition, we have shown how MASML reactions under equimolar reagent concentrations outperform non-MASML reactions employing excess reagents, and demonstrated how secondary bioorthogonal ligation reactions can be performed on MASML products without the need for intermediate purification steps.

In total, these studies demonstrate how MASML is an effective and easily implemented strategy for improving SML methodology.

2. Preparation of Protein Targets and Peptide Nucleophiles

2.1 Design, Expression and Purification of MASML Protein Substrates

As described above, the intention of this study was to demonstrate the applicability of MASML to full size protein targets. To this end, we identified a variety of small protein targets to use as MASML substrates. The panel of chosen substrates included DARPin and affibody molecules, both with high HER2 binding affinity.[53,54] The DARPin (designed ankyrin repeat protein) structure is based on the common ankyrin repeat motif which facilitates protein-protein interactions through the loops between helices (**Figure 8a**), and can be specifically engineered to bind a wide range of complementary antigens.[55] Affibody molecules (**Figure 8b**) are based on the immunoglobulin G binding domain of protein A, and can be given novel binding specificity via directed evolution, similar to DARPin.[56] This study also included a monobody molecule specific for YES1,[57] a tyrosine kinase involved in the regulation of cell growth and survival; as well as a fynomer complementary to a serine protease chymase involved in allergic reactions.[58]

Monobodies (**Figure 8c**) are another type of antibody mimetic, built using the fibronectin type III domain as a scaffold.[59] Fynomer (**Figure 8d**) is based on the SH3 domain of the tyrosine-protein kinase Fyn, which is generally associated with cell signaling.[60] The final substrate used in this thesis was a commercially available solubility tag, Fh8,[61] equipped with a MASML-compatible linker.

In all cases other than Fh8, protein targets were examples of non-antibody scaffolds for molecular recognition and are regarded as promising alternatives to full size antibodies for the development of therapeutics and basic research tools.[62] Notably, SML has previously been shown to be an effective tool for appending secondary functionality to antibodies, including fluorophores and therapeutics.[9,11,18,27,44] The rising interest in non-antibody scaffolds therefore makes these proteins high value targets for the development of site-specific modification strategies such as MASML.

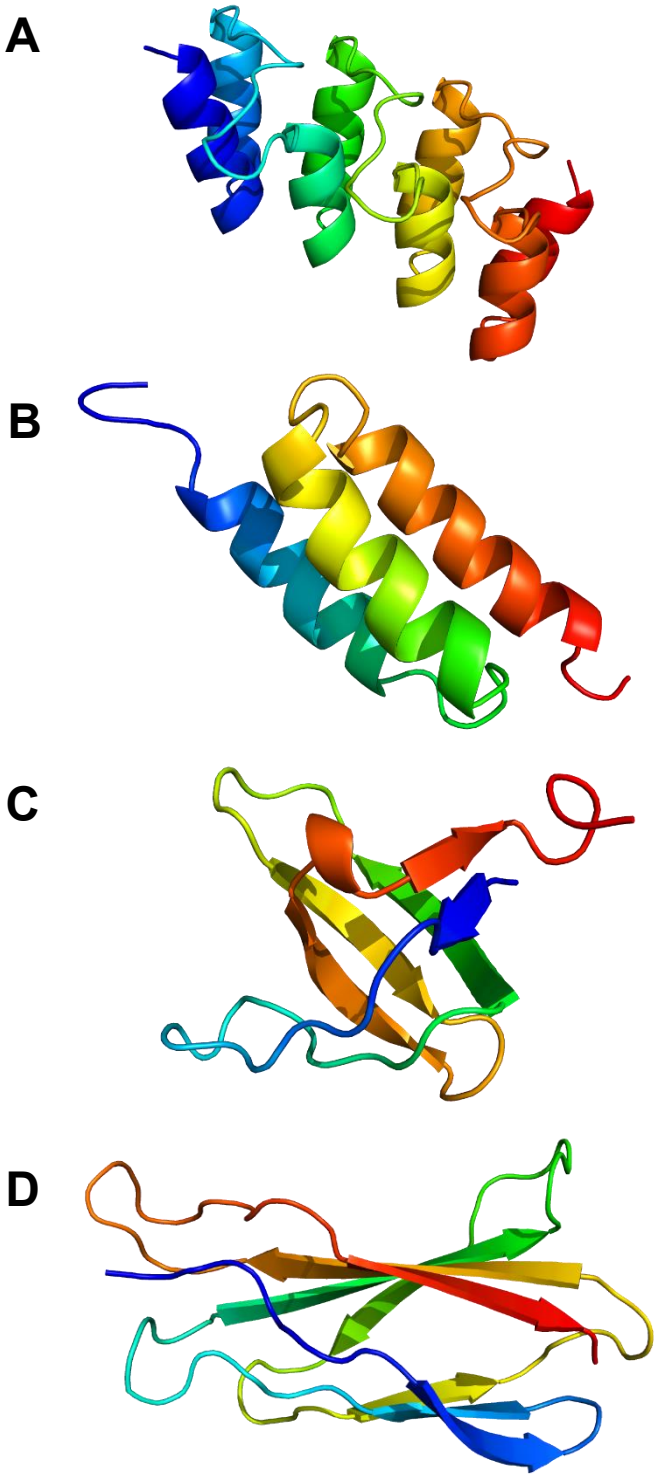

Figure 8. Crystal structures of the protein substrates used in this study. (A) DARPin with affinity for HER2, PDB: 2JAB. (B) Affibody with affinity for HER2, PDB: 2KZJ. (C) Fynomer with affinity for serine protease chymase, PDB: 4AFS. Monobody with affinity for YES1, PDB: 5MTJ.

To render the protein targets compatible with MASML, all proteins were produced with sortase-ready C-termini, containing a short spacer ($(G_4S)_2$) followed by the sortase recognition sequence (LPETGG), and ending in a His_6 tag (**Figure 9**). This arrangement allows for nesting of the nickel-binding GGH motif directly into the sortase and His_6 sites. Plasmids encoding these constructs were obtained via commercial gene synthesis. To designate the presence of the sortase-ready C-termini, these protein substrates are hereafter designated sDARP, sAff, sMon, sFyn and sFh8.

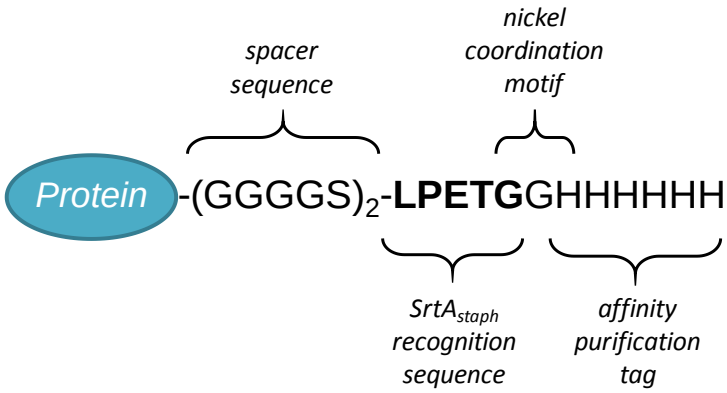

Figure 9. General structure of MASML-compatible protein substrates used in this study.

The plasmids were transformed into BL21(DE3) *E. coli* cells and protein production was performed using standard IPTG-induced overexpression. After lysing the cells and separating out the protein containing lysate, all proteins were purified using the same two step method. First, the proteins were IMAC purified on a gravity flow-based Ni-NTA column to remove the majority of contaminants. The elutions were then desalted using an FPLC system, and the fractions combined for a secondary IMAC purification step. This second IMAC step was found to remove non-target protein contaminants, but the main purpose was to separate out truncated variants of the target proteins. These variants typically lacked two of the histidines from the His_6-tag and were visible in post-desalting

analysis via ESI-MS (**Figure 10**). These His_4 proteins could be separated by FPLC-based Ni-NTA purification, using a controlled gradient of imidazole buffer to elute the variants at different times. Fractions were examined using ESI-MS and those containing only His_6 were combined and desalted. Final ESI-MS analysis revealed proteins of at least 95% purity in all cases, at which point the substrate proteins were ready for use in MASML reactions (see **Appendix III** for analytical ESI-MS spectra and SDS-PAGE of each protein stock solution).

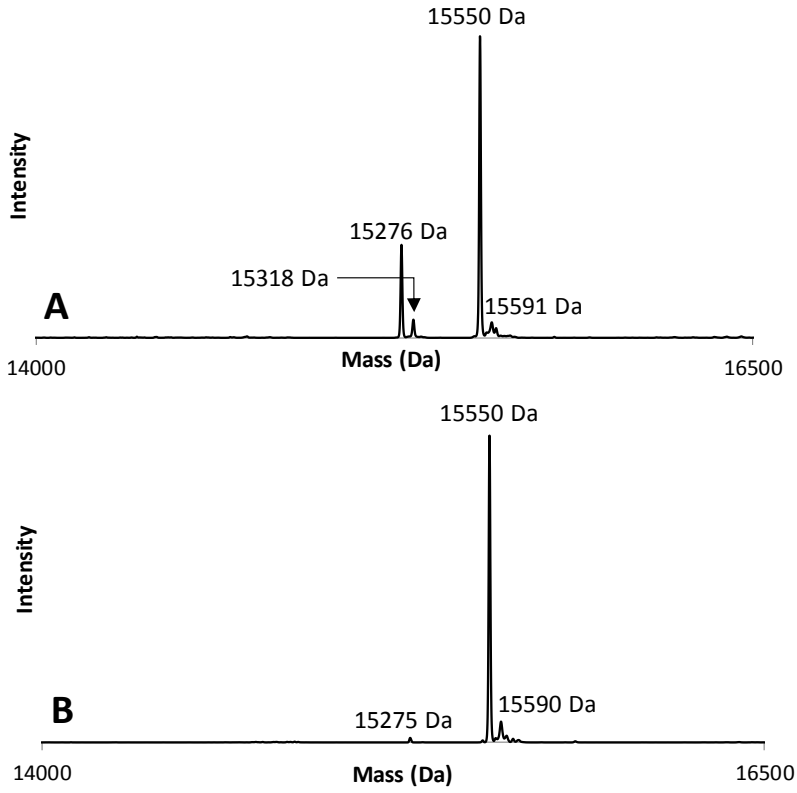

Figure 10. ESI-MS spectra of sDARP after the first **(A)** and second **(B)** IMAC purification steps. Expected mass for the full protein was 15550 Da, while the His_4 variant had an expected mass of 15276 Da. Minor contaminants including the addition of ~40-42 Da are postulated to correspond to acetylated protein derivatives.

2.2 Synthesis of MASML-Compatible Nucleophile Library

Similar to the protein substrates, the nucleophile library generated for this research was created with a focus on installing modifications of proven industrial and medical use. To begin with, three common fluorophores were selected: 6-carboxyfluorescein (6-FAM), cyanine-3 (Cy3), and 7(diethylamino)courmarin-3-carboxylic acid (DEAC). In addition, a branched polyethylene glycol chain with a discrete mass of 2190 Da (dPEG2000) was used as well. The final modification was an established click-handle, dibenzocyclooctyne (DBCO). These functional groups were chemically appended to the lysine side-chain of a small base peptide, generated through standard solid phase peptide synthesis (SPPS) methods. The base peptide had the sequence GGK for all nucleophiles except the PEGylated variant, which contained an additional tyrosine residue for quantification, as PEG does not possess an easily quantified chromophore. The full structure of all MASML-compatible peptides used in this thesis are given in **Figure 11.**

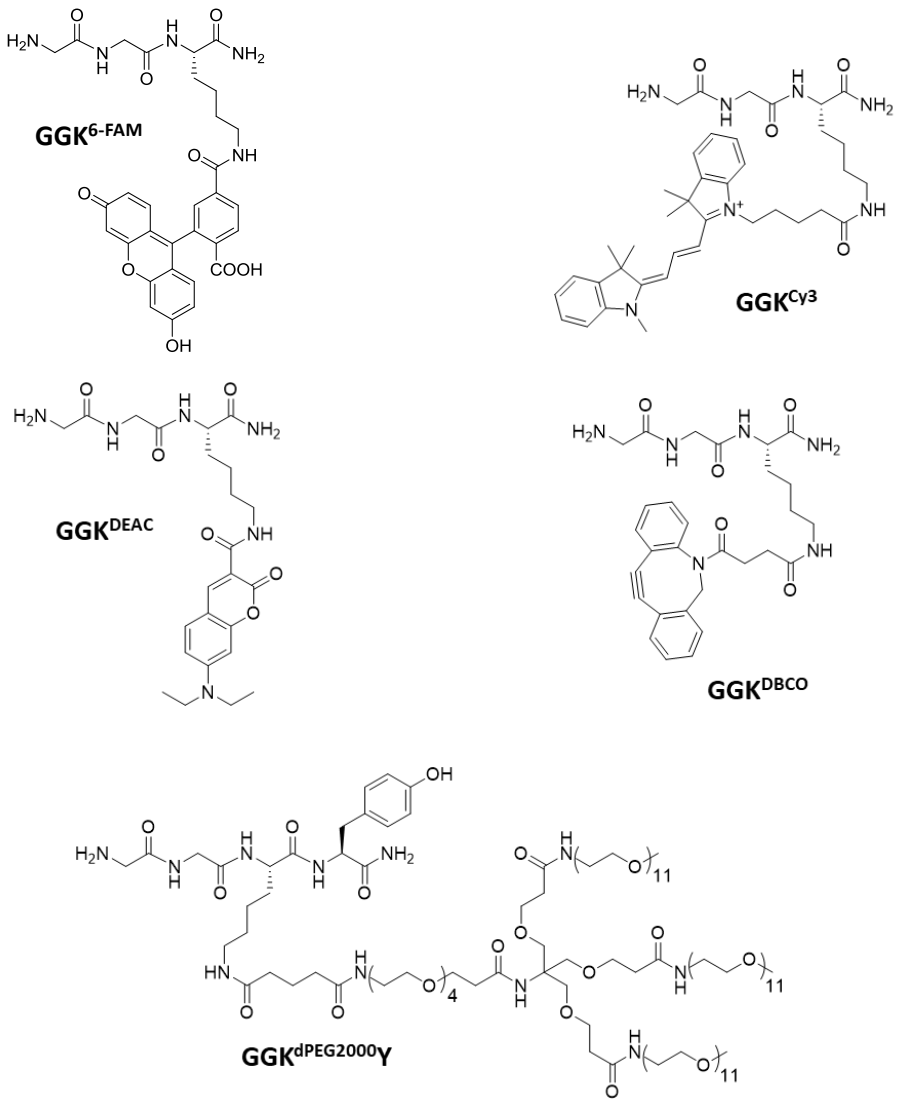

Figure 11. Structures of nucleophiles and appended modifications used in this study.

The preparation of all nucleophiles was achieved using a similar strategy. As illustrated in **Figure 12**, a base peptide was first generated by SPPS and then cleaved from the resin without a final deprotection step so as to leave the N-terminus Fmoc-protected. The identities of the base peptides were confirmed by ESI-MS. Crude peptide solutions were then combined with the desired modification, activated as the corresponding N-hydrozysuccinimide (NHS) ester or tetrafluorophenol (TFP) ester. A 2-fold molar excess of the base peptide was employed to ensure complete consumption of

the activated esters. These coupling steps were monitored using ESI-MS (**Figure 13**), and upon completion, piperidine was added to remove the Fmoc group, deprotecting the N-terminus. Final nucleophile products were purified using by RP-HPLC. Product identity and purity were confirmed using ESI-MS and HPLC analysis, respectively (**Appendix II**). The completed nucleophiles were quantified using the extinction coefficient of their respective functional groups (tyrosine in the case of GGK^{dPEG2000}Y). Approximately 1mM stocks of each nucleophile were prepared for use in later MASML reactions.

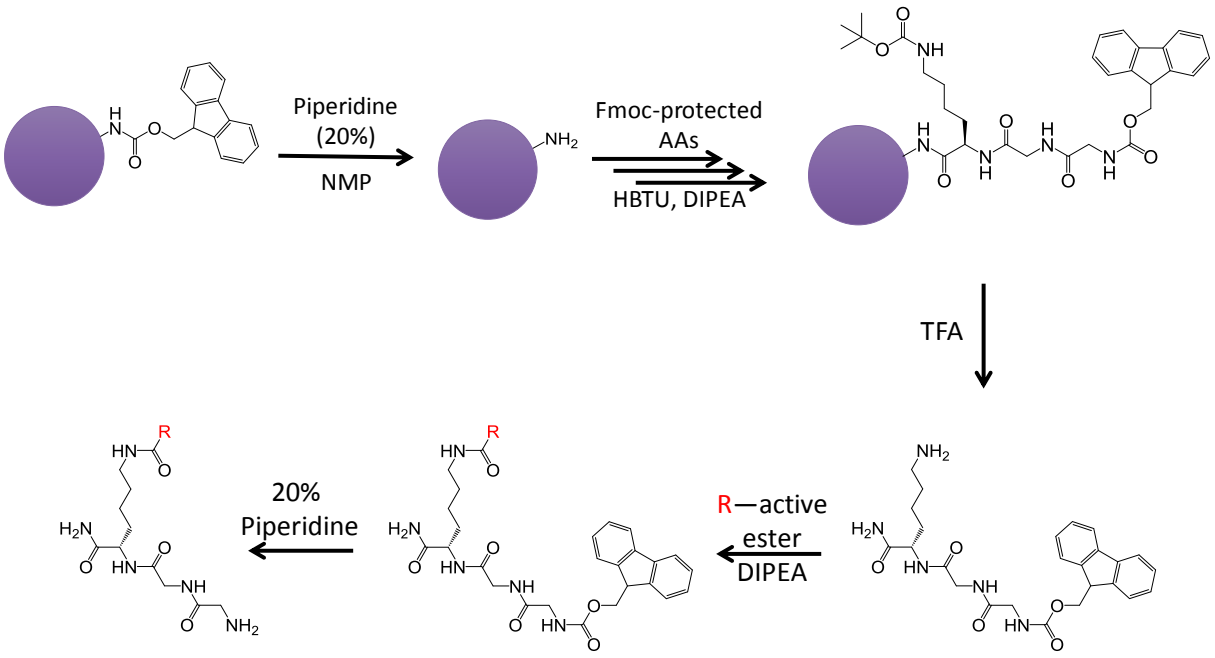

Figure 12. Representative synthesis scheme for the generation of peptide nucleophiles used in this study.

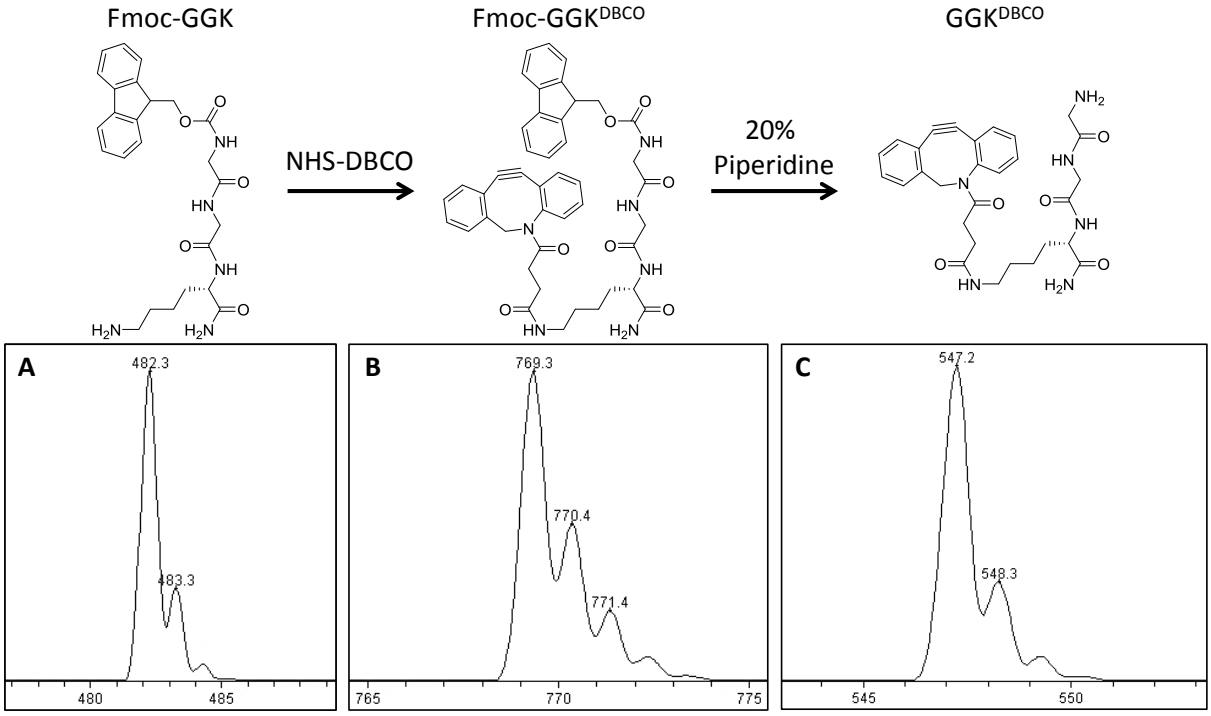

Figure 13. Representative ESI-MS spectra for the synthesis of GGK^{DBCO}: **(A)** Fmoc-GGK base peptide, **(B)** ligation of Fmoc-GGK with NHS-DBCO, **(C)** final ESI-MS analysis of the GGK^{DBCO} stock following Fmoc deprotection and HPLC purification. Expected $[M+H]^+$ values: Fmoc-GGK = 482.2 Da, Fmoc-GGK^{DBCO} = 769.3 Da, GGK^{DBCO} = 547.3 Da.

3. Results

3.1 C-terminal Fluorophore Labeling of DARPin

With all necessary reagents in hand, we proceeded to investigate the compatibility of MASML with different protein targets and modifications. In all cases, it was anticipated MASML would give significant improvements in ligation efficiency when equimolar concentrations of the protein substrates and glycine nucleophiles were combined in the presence of a Ni^{2+} additive. Furthermore, we sought to demonstrate these MASML reactions would significantly outperform the corresponding control reactions lacking Ni^{2+}.

To begin, we established a standard set of reaction conditions consisting of 50μM of each ligation partner, and 10 μM $SrtA_{Staph}$ (**Figure 14**). For Ni^{2+}, a 4-fold molar excess

(relative to protein substrate) of $NiSO_4$ was found in preliminary studies with sDARP to give significant improvements in sortase-mediated ligation conversion with no apparent deleterious effects on protein solubility. Higher Ni^{2+} concentrations were prone to protein precipitation and failed to further improve ligation efficiency. All reactions were conducted at room temperature.

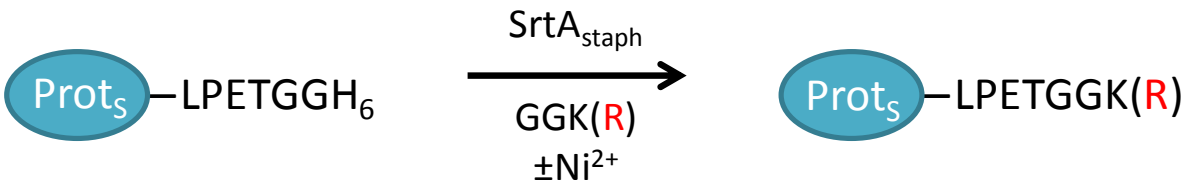

Figure 14. Overview of C-terminal modification via MASML.

Conjugation of sDARP and GGK$^{6\text{-FAM}}$. In the initial reaction system, the C-terminal modification of sDARP with GGK$^{6\text{-FAM}}$ was performed in the presence or absence of Ni^{2+} and monitored over the course of 9 hours (**Figure 15a**). All reactions were performed in duplicate and monitored using ESI-MS to track the relative concentrations of unmodified starting material and conjugated product. Reconstructed mass spectra were used to estimate the relative amounts of all proteins species, including any hydrolyzed starting material arising from hydrolysis of the acyl-enzyme intermediate (**Figure 15**).

The (-)Ni^{2+} reactions reached completion at 6 hours, and achieved a maximum conversion of 41%, while the (+)Ni^{2+} reactions reached completion at 8 hours, with a final conversion of 84%. Hydrolysis was observed to increase for the (+)Ni^{2+} reactions, with an increase from <1% to 9.5% with the addition of Ni^{2+}.

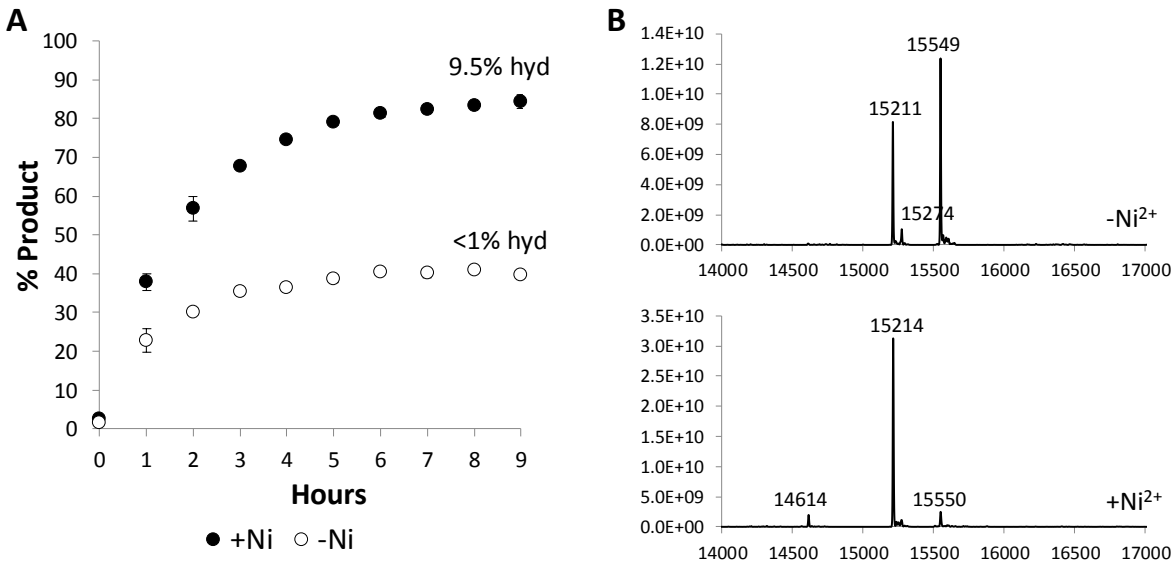

Figure 15. ESI-MS time course data for the C-terminal modification of sDARP with $GGK^{6\text{-}FAM}$. (**A**) Product conversion for both reactions as estimated by ESI-MS. All data points represent the mean of duplicate trials, with error bars corresponding to the full range of the data set. (**B**) ESI-MS spectra from the 9hr timepoints of the $(+)Ni^{2+}$ (bottom) and $(-)Ni^{2+}$ (top) reactions (calculated molecular weights: sDARP = 15550 Da, sDARP(6-FAM) = 15213 Da, hydrolyzed sDARP = 14613 Da).

Conjugation of sDARP and GGK^{Cy3} / GGK^{DEAC}. To evaluate compatibility with other fluorophores, we proceeded to investigate the ligation of GGK^{Cy3} and GGK^{DEAC} using the same DARPin substrate. Reactions were identical to those described above, and were monitored by ESI-MS over the course of 9 hours. Interestingly, in the case of Cy3 the $(-)Ni^{2+}$ reactions performed surprisingly well, and reached completion at 7 hours with a maximum product conversion of 77% (**Figure 16a**). The $(+)Ni^{2+}$ reactions did give improved results, reaching completion at around 8 hours, with a final conversion of 95% (**Figure 16b**). Hydrolysis was only minorly enhanced in the $(+)Ni^{2+}$ reactions, with an increase from <0.5% to ~1% (estimated by mass spectrometry) with the addition of Ni^{2+}. While the enhancement provided by Ni^{2+} was less pronounced for this reaction than for the ligation of sDARP and $GGK^{6\text{-}FAM}$, there was no overlap in the two datasets, implying

some enhancing effect by Ni^{2+} on the reaction efficiency. This reaction may simply represent a case where the ligation equilibrium is inherently biased towards products, potentially due to the properties of the Cy3 dye. This phenomenon was not investigated further.

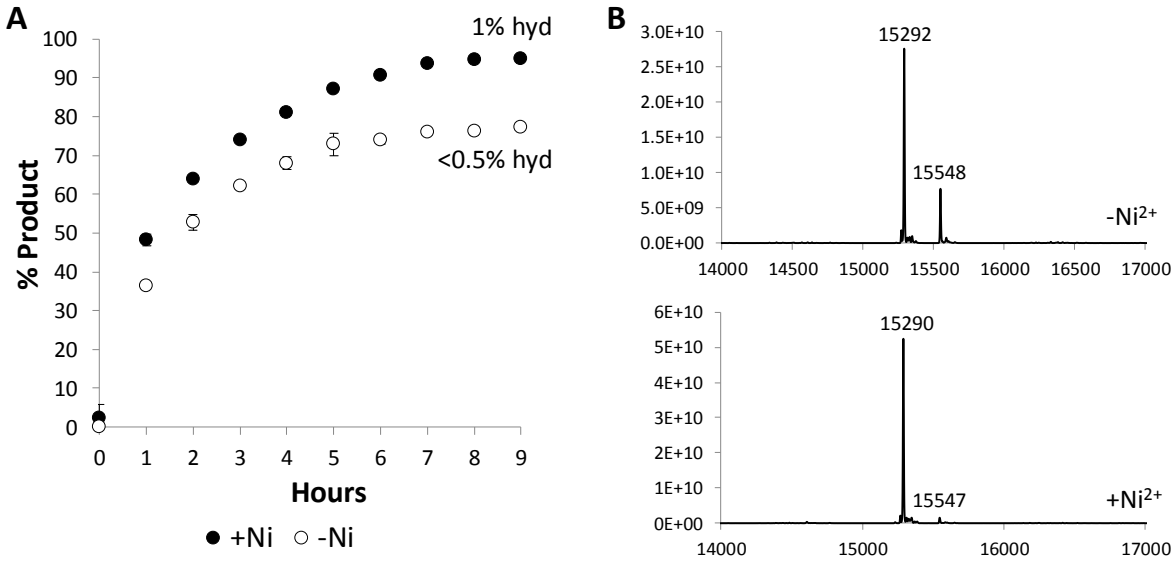

Figure 16. ESI-MS time course data for the C-terminal modification of sDARP with GGK^{Cy3}. (**A**) Product conversion for both reactions was estimated by ESI-MS. All data points represent the mean of duplicate trials, with error bars corresponding to the full range of the data set. (**B**) ESI-MS spectra from the 9hr timepoints of the (+)Ni^{2+} (bottom) and (-)Ni^{2+} (top) reactions (calculated molecular weights: sDARP = 15550 Da, sDARP(Cy3) = 15291 Da).

Moving on to the ligation of the DEAC-functionalized nucleophile, Ni^{2+} was once again found to significantly improve reaction efficiency when monitored over the course of 12 hours (**Figure 17a**). The (+)Ni^{2+} trials were observed to run at a slower initial rate than the (-)Ni^{2+} reactions, unlike the previous MASML reactions performed for sDARP with $GGK^{6\text{-}FAM}$ and GGK^{Cy3}. The (+)Ni^{2+} reactions were therefore repeated (4 trials total) to confirm this trend, which was observed in all trials including Ni^{2+}. Despite this initial delay in reaction progress, ligation in the presence of Ni^{2+} ultimately provided superior reaction conversions. Specifically, the (-)Ni^{2+} reactions reached completion at 9 hours and

achieved a maximum product conversion of 65%, while the (+)Ni^{2+} reactions were seemingly still slowly proceeding at 12 hours, having reached a conversion of 94% (**Figure 17a**). Hydrolysis was minimal in all reactions, reaching a maximum of 2.5% when ligations were run in the presence of Ni^{2+}.

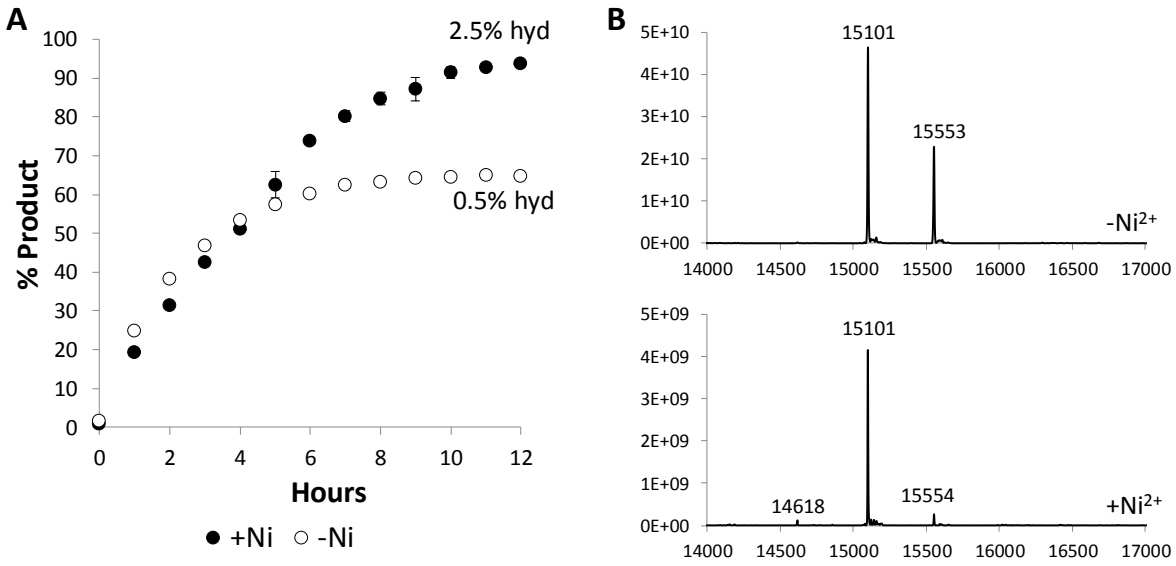

Figure 17. ESI-MS data for the C-terminal modification of sDARP with GGK^{DEAC}. (**A**) Product conversion for both reactions was estimated by ESI-MS. All data points represent the mean of duplicate trials, with error bars corresponding to the full range of the data set. (**B**) ESI-MS spectra from the 12hr timepoints of the (+)Ni^{2+} (bottom) and (-)Ni^{2+} (top) reactions (calculated molecular weights: sDARP = 15550 Da, sDARP(DEAC) = 15098 Da, hydrolyzed sDARP = 14613 Da).

Comparison of MASML to SML with Excess Reagent Loading. To further demonstrate the enhancement of ligation efficiency provided by MASML, we next compared the results of ligations using a MASML approach to those of a standard SML strategy in which excess glycine nucleophile was used to drive the reaction to completion. To this end, the SML reaction of sDARP and GGK^{DEAC} in the absence of Ni^{2+} was investigated using varied loadings of nucleophile (2, 3, 5 and 20 molar equivalents). The reactions were monitored over the course of 11 hours, and the results were compared to the initial (+)Ni^{2+} and (-)Ni^{2+} trials for equimolar concentrations of starting material (**Figure**

18a). Remarkably, even with a 20-fold excess of GGK^{DEAC} the reactions lacking Ni^{2+} failed to outperform the corresponding MASML reaction using only 1 molar equivalent of GGK^{DEAC}. Specifically, the MASML reaction with one equivalent of GGK^{DEAC} gave conversions of ~93% at the 11hr timepoint, while the (-)Ni^{2+} reaction with 20 equivalents of GGK^{DEAC} reached ~90% (**Figure 18a**). Ligation yields were continuously improved with each consecutive increase in nucleophile concentration in the absence of Ni^{2+}, however there was an gradual decrease in the enhancement effect of each additional equivalent of nucleophile. For example, the increase in yields when going from 3x to 5x (3.7%) was the same as the increase when going from 5x to 20x (3.6%). Overall, these results showed the MASML approach significantly improved reaction efficiency, allowing for reduced loading of the GGK^{DEAC} nucleophile without negatively impacting the production of ligation products.

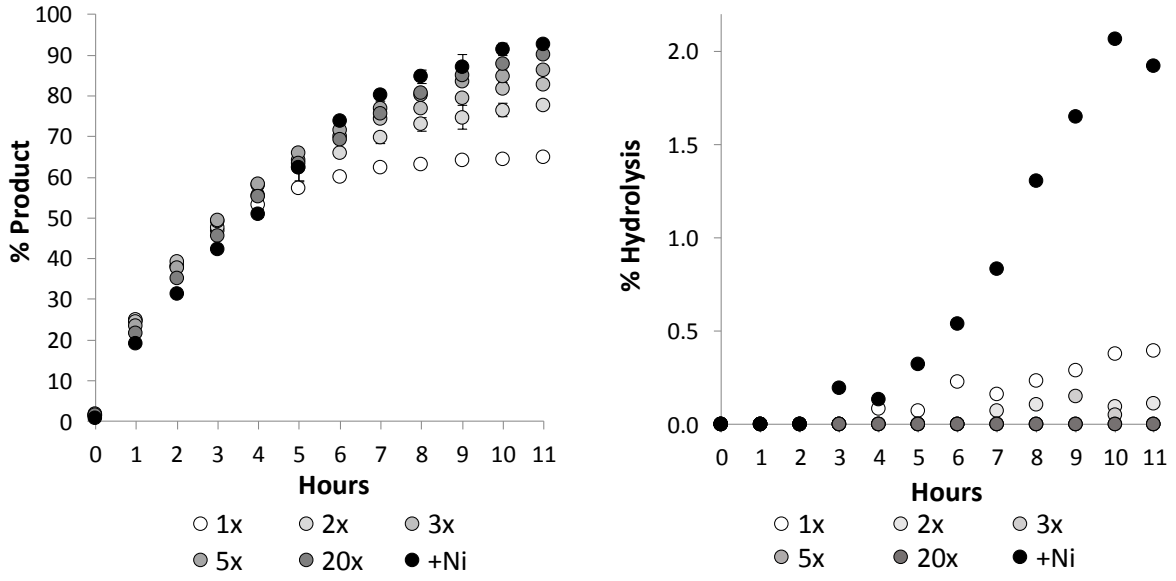

Figure 18. ESI-MS data for the C-terminal modification of sDARP with varied loadings of GGK^{DEAC} in the presence or absence of Ni^{2+}. The reaction with Ni^{2+} was only performed using one equivalent of GGK^{DEAC}. (**A**) Product conversion as estimated by ESI-MS for all (-)Ni^{2+} reactions (1-20 equivalents of GGK^{DEAC} as well as the original (+)Ni^{2+} reaction with one equivalent of GGK^{DEAC}). All data points represent the mean of two trials, with error bars corresponding to the full range of the data set. (**B**) Hydrolysis product concentration averaged for the same data sets as in **A**.

Hydrolysis was also affected by increasing the nucleophile concentration (**Figure 18b**). As the amount of nucleophile available increased, the amount of hydrolysis decreased, likely due to the excess nucleophile outcompeting water for reaction with the acyl-enzyme intermediate. Hydrolysis became negligible by 2 equivalents of GGK^{DEAC} (<0.5%) and was completely undetectable in reactions with 20 equivalents of GGK^{DEAC}. While the reactions containing Ni^{2+} did result in the highest levels of hydrolysis (~2%), the MASML approach was clearly superior in terms of ligation product formation and eliminated the need for excess nucleophile in the ligation reaction (**Figure 19**).

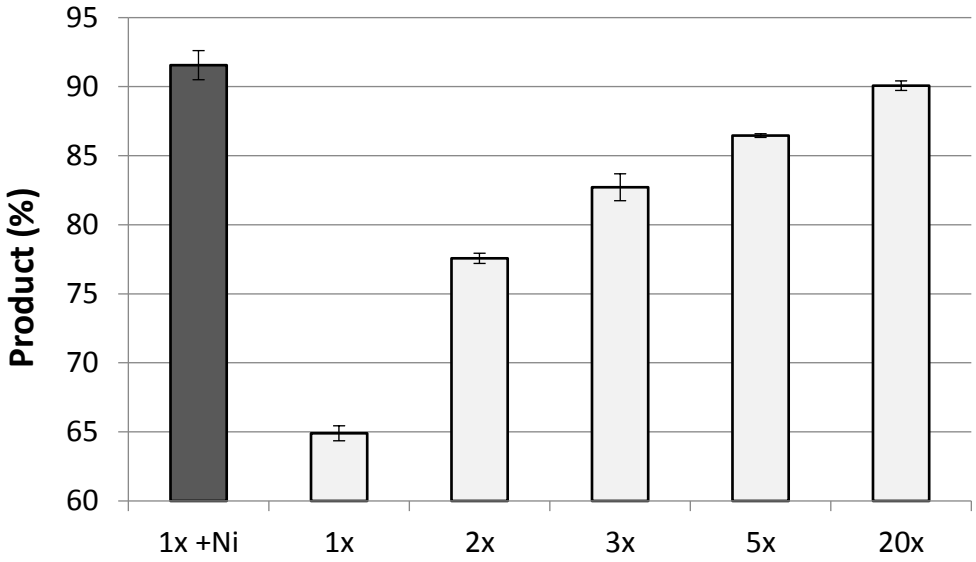

Figure 19. Endpoint (11hr) product conversion amounts for the various (-)Ni^{2+} reactions (light gray columns), compared to the initial (+)Ni^{2+} reactions using one molar equivalent of GGK^{DEAC} (dark gray column). Labels below chart indicate the equivalents of GGK^{DEAC} used. Product formation (%) was estimated by ESI-MS.

3.2 C-terminal Modification of Protein Substrates with DEAC

Conjugation of sAff and GGK^{DEAC}. Having investigated the ligation of multiple fluorophores to sDARP using MASML, we next turned our attention to other protein targets, beginning with the C-terminal modification of sAff with GGK^{DEAC}. Reactions were performed in the presence or absence of Ni^{2+} for 12 hours and monitored by ESI-MS

(**Figure 20a**). Surprisingly, sAff proved to be a poor substrate, with yields never exceeding 30% in either the presence or absence of Ni^{2+} (**Figure 20a**). Hydrolysis of sAff was not detected for the (-)Ni^{2+} reaction, and did not exceed 0.5% with the addition of nickel. While the reason for the poor reactivity of sAff remains unclear, we do note a similar affibody-based SML substrate has been described in the literature, and poor reactivity was observed in this report as well.[63] Therefore, the LPXTG substrate site on the affibody may require additional engineering and optimization to improve reactivity. This substrate was not investigated further.

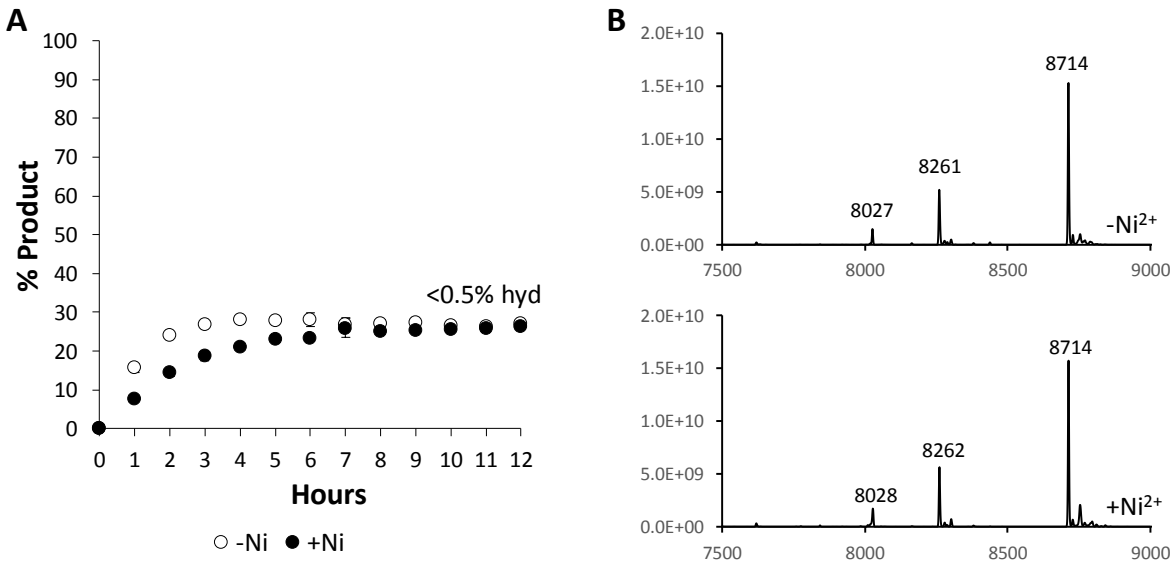

Figure 20. ESI-MS data for the C-terminal modification of sAff with DEAC. (**A**) Product conversion for both reactions was estimated by ESI-MS. All data points represent the mean of duplicate trials, with error bars corresponding to the full range of the data set. (**B**) ESI-MS spectra from the 12hr timepoints of the (+)Ni^{2+} (bottom) and (-)Ni^{2+} (top) reactions (calculated molecular weights: sAff = 8714 Da, sAff(DEAC) = 8261 Da, sAff-His_1 = 8027 Da).

Conjugation of sFyn and GGK^{DEAC}. The C-terminal modification of sFyn with DBCO was next analyzed in the presence or absence of Ni^{2+} for 12 hours (**Figure 21a**). The (-)Ni^{2+} reaction reached completion at 8 hours and achieved a maximum product conversion of 44%, while the (+)Ni^{2+} reaction reached completion at 9 hours, with a final

yield of 94% (**Figure 21b**). Hydrolysis was negligible for both reactions, with concentrations below 1% for the (+)Ni^{2+} reactions, and no detectable hydrolysis until the 11 hour timepoint of the (-)Ni^{2+} reactions.

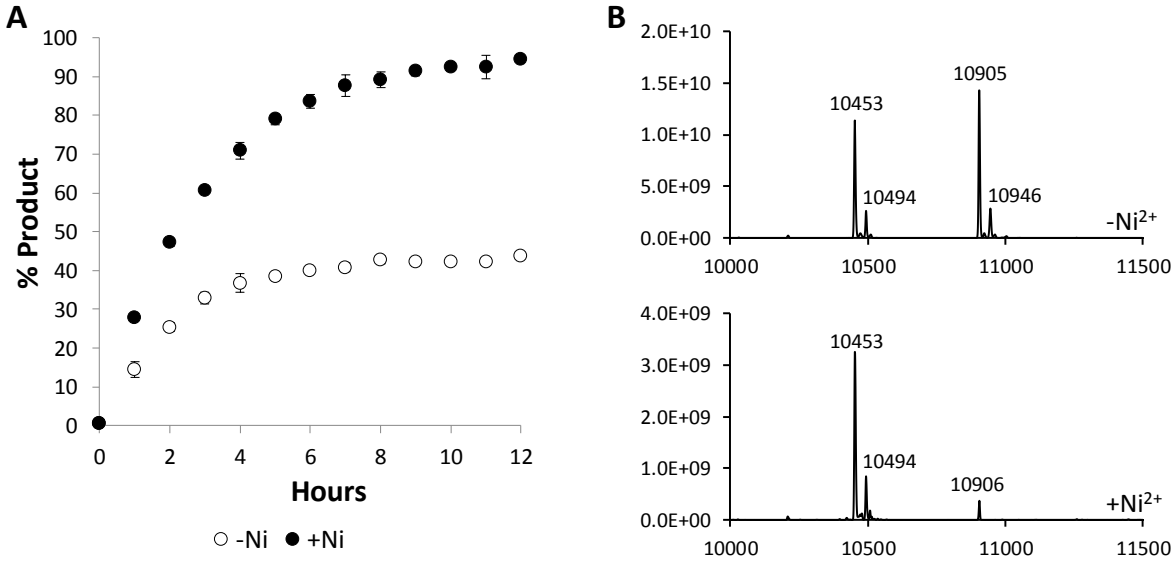

Figure 21. ESI-MS data for the C-terminal modification of sFyn with DEAC. (**A**) Product conversion for both reactions was estimated by ESI-MS. All data points represent the mean of duplicate trials, with error bars corresponding to the full range of the data set. (**B**) ESI-MS spectra from the 12hr timepoints of the (+)Ni^{2+} (bottom) and (-)Ni^{2+} (top) reactions (calculated molecular weights: sFyn = 10907 Da, sFyn(DEAC) = 10454 Da, putative acetylation of protein substrate resulted in peaks of approximately +41 Da).

Conjugation of sMon and GGK^{DEAC}. The C-terminal modification of sMon with DEAC was investigated next. The sMon substrate proved to be somewhat more challenging as the standard 4 molar equivalents of Ni^{2+} used for other protein targets led to sMon precipitation. To circumvent this issue, we reduced Ni^{2+} to 2 equivalents, and included 20% (v/v) DMSO to promote sMon solubility. ESI-MS analysis was also difficult as sMon displayed low ionization efficiency, and so reactions were instead analyzed via SDS-PAGE (**Figure 22**). Aliquots of the (+)Ni^{2+} or (-)Ni^{2+} reactions were collected at 0, 6, 12, and 24hrs and quenched with 4x DTT and SDS containing loading buffer. The (-)Ni^{2+}

reaction achieved a product conversion of 43% after 6 hours, and a maximum conversion of 65% after 12hrs, while the (+)Ni^{2+} reactions reaction a conversion to product of 70% by 6hrs, and a final yield of 85% at 12hrs (**Figure 22**). Hydrolysis was not detected for either reaction. An additional reaction lacking both nickel and DMSO was run as a control. This reaction progressed marginally faster than the (-)Ni^{2+} reaction, but did not exceed the (+)Ni^{2+} reaction, with a 6hr yield of 61% and final yield of 68%. From this control dataset we concluded the addition of DMSO likely slowed the overall rate of the reaction, but likely did not impact the final yield amounts.

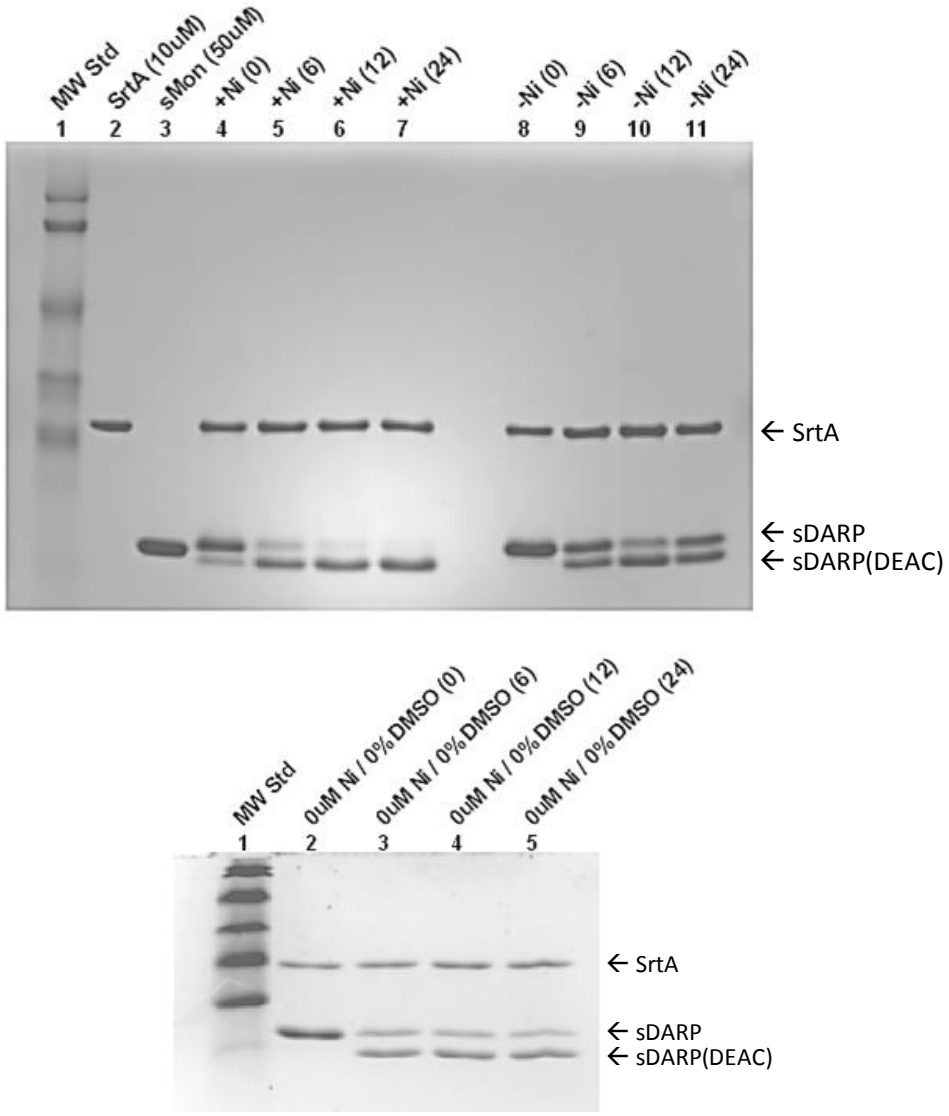

Figure 22. SDS-PAGE gels for the C-terminal modification of sMon with DEAC. (Top) Lane 1 contains a molecular weight standard, lanes 2 and 3 contain standards of $SrtA_{Staph}$ and sMon respectively, at reaction concentrations. Lanes 4-7: (+)Ni^{2+} reaction (20% DMSO) at 0, 6, 12, and 24hrs. Lanes 8-11: (-)Ni^{2+} reaction (20% DMSO) at 0, 6, 12, and 24hrs. (Bottom) Lane 1: molecular weight standard; lanes 2-5: control reaction containing no Ni^{2+} and no DMSO, at 0, 6, 12 and 24hrs.

Conjugation of sFh8 and GGK^{DEAC}. As a final protein target, we explored the C-terminal modification of sFh8 with GGK^{DEAC} in the presence or absence of Ni^{2+} over the course of 12 hours (**Figure 23a**). As observed in the case of sDARP and GGK^{Cy3}, the (-)Ni^{2+} reactions were observed to be surprisingly successful and exhibited 79%

conversion to the ligation product after 12 hours. While successful, the (-)Ni^{2+} reaction was outperformed by the (+)Ni^{2+} system, which reached 96% conversion over the same time period (**Figure 23b**). Hydrolysis was not detected for either reaction.

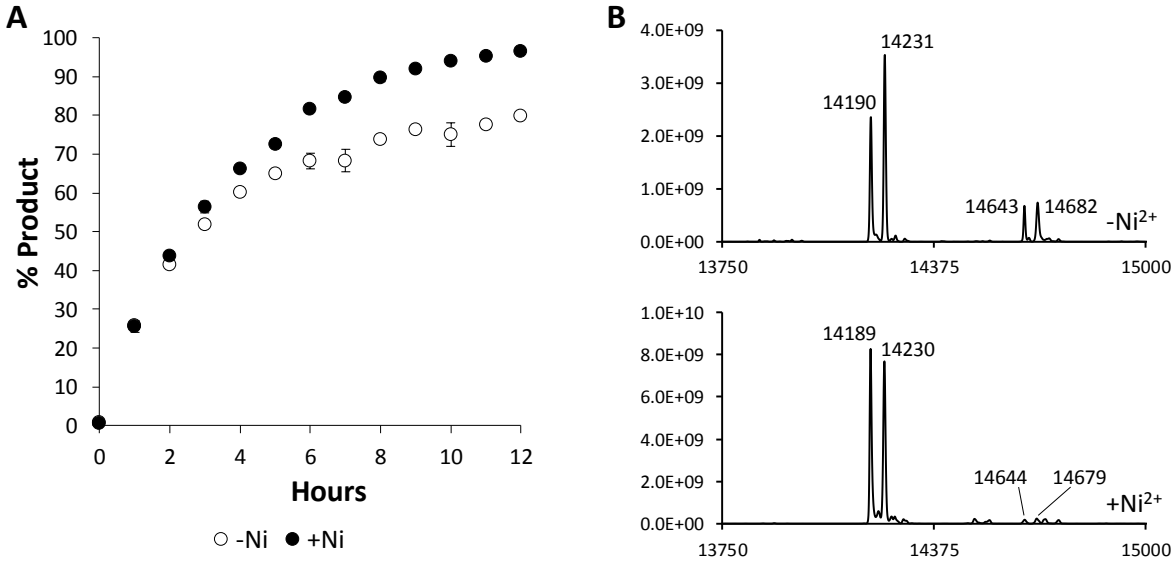

Figure 23. ESI-MS data for the C-terminal modification of sFh8 with DEAC. (**A**) Product conversion for both reactions was estimated by ESI-MS. All data points represent the mean of duplicate trials, with error bars corresponding to the full range of the data set. (**B**) ESI-MS spectra from the 12hr timepoints of the (+)Ni^{2+} (bottom) and (-)Ni^{2+} (top) reactions (calculated molecular weights: sFh8 = 14636 Da, sFh8(DEAC) = 14183 Da, putative acetylation of protein substrate resulted in peaks of approximately +41 Da).

3.3 C-terminal PEGylation of DARPin using MASML

To further investigate the scope of modifications that were compatible with MASML, we evaluated the attachment of a branched, monodisperse PEG chain (dPEG2000) to sDARP. The attachment of PEG and polymers using sortase has been reported, and therefore this represents an important area of interest for users of sortase-based methods.[64] As described in **Section 2.2**, the nucleophile for this application contained a GGKY base peptide tethered to the branched PEG via an amide linkage to the lysine side-chain. One molar equivalent of this nucleophile was combined with sDARP

in the presence or absence of Ni^{2+} and monitored for 12 hours by ESI-MS (**Figure 24a**). As anticipated, a marked improvement in ligation efficiency was observed when Ni^{2+} was included. Specifically, the (-)Ni^{2+} reactions reached completion at 5 hours and achieved a maximum conversion of 48%, while the (+)Ni^{2+} reactions reached completion at 10 hours, with a substantially improved final yield of 91% (**Figure 24b**). It should be noted the ESI-MS signal for the PEG conjugated sDARP contained significant levels of ammonium adducts, which has been observed previously for PEG conjugates.[65] The signal from these ammonium adducts was included in the calculations for reaction conversion. In addition to an increase in PEG attachment, hydrolysis was observed to slightly increase for the (+)Ni^{2+} reactions, with an increase from <1% to 3.5% with the addition of Ni^{2+}.

These reactions were also examined by SDS-PAGE (**Figure 25**). Aliquots of the (+)Ni^{2+} and (-)Ni^{2+} reactions were collected at 0, 4.5, and 9 hours and quenched by the addition of reducing SDS-PAGE loading buffer. Samples were then analyzed by SDS-PAGE along with control lanes containing $SrtA_{Staph}$ and unmodified sDARP (both at final reaction concentrations). Relative band intensities from the Coomassie stained gel were used to estimate product conversion at each time point. An improvement in reaction conversion was observed when Ni^{2+} was included. The (-)Ni^{2+} reaction was finished by 4.5 hours with a maximum conversion below 50%, while the (+)Ni^{2+} reaction was still progressing at 4.5 hours and had reached 70% conversion by the final timepoint. While the conversion amounts calculated from the gel do not exactly match those seen in the ESI-MS data, the overall trends remained consistent.

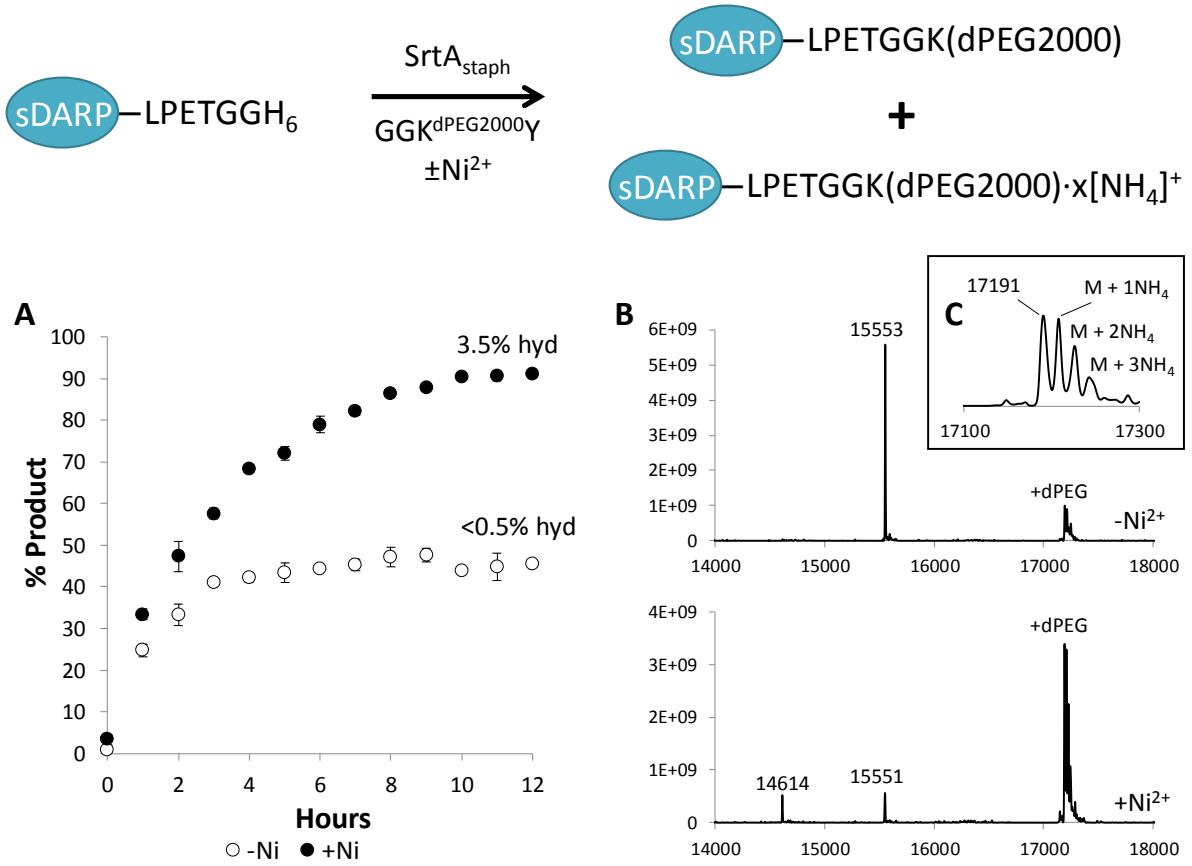

Figure 24. (Top) Reaction scheme depicting the PEGylation of DARPin via MASML. (Bottom) ESI-MS data for the C-terminal modification of sDARP with GGK^{dPEG2000}Y. (**A**) Product conversion for both reactions was estimated by ESI-MS. All data points represent measurements averaged over two trials, with error bars corresponding to the full range of the data set. The total signal for the sDARP(dPEG2000) conjugate was the summation of the parent mass (M) as well as the observed ammonium adducts. (**B**) Example ESI-MS spectra from the 12hr timepoints of the (+)Ni^{2+} (bottom) and (-)Ni^{2+} (top) reactions (calculated molecular weights: sDARP = 15550 Da, sDARP(dPEG2000) = 17190 Da, hydrolyzed sDARP = 14613 Da). **(C)** Close-up view of PEG conjugated sDARP from the (-)Ni^{2+} reaction showing presence of ammonium adducts (+18 Da).

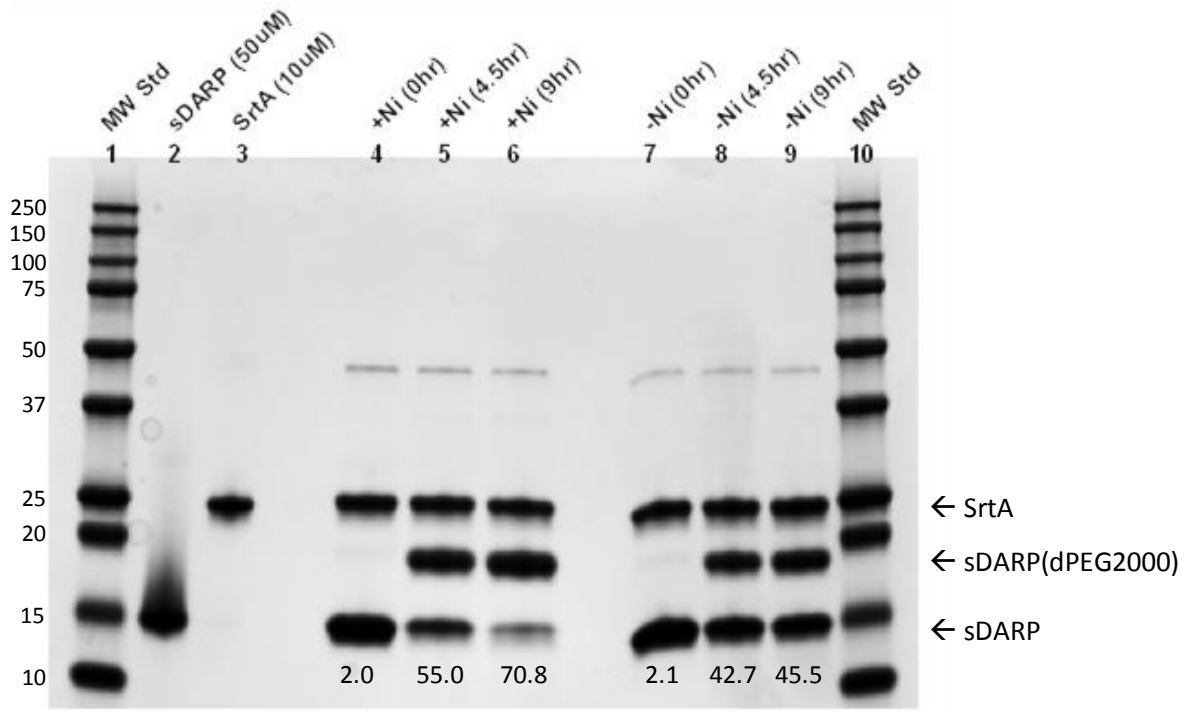

Figure 25. SDS-PAGE analysis of the C-terminal modification of sDARP with dPEG2000, in the presence or absence of Ni^{2+}. Lane 1: Molecular weight standard with masses (kDa) labeled. Lane 2: Control containing only sDARP at 50μM. Lane 3: Control containing only $SrtA_{Staph}$ at 10μM. Lanes 4-6: Timepoints for the (+)Ni^{2+} reaction. Lanes 7-9: Timepoints for the (-)Ni^{2+} reaction. Lane 10: Molecular weight standard. Percent conversion values, estimated from relative band intensities, are indicated at the bottom of each lane.

3.4 Combined MASML and Bio-orthogonal Ligation

Bioorthogonal ligation reactions, or “click” reactions, have garnered significant attention for their ability to facilitate rapid, covalent ligations, which can be performed on organic and inorganic molecules alike, using mild reaction conditions.[66,67] Copper-free click chemistry is of particular import, as it eliminates the copper catalyst typically required for azide-alkyne click reactions, which can be detrimental to live-cell applications. These reactions occur in the absence of a catalyst by introducing strain to the alkyne, commonly in the form of a cyclooctyne.[68] When introduced into the same reaction mixture, the click handles undergo a Huisgen cyclization to produce the ligation product (**Figure 26**). These

handles can be readily appended to proteins and peptides via NHS-ester chemistry, thus allowing for the rapid generation of complex molecules.

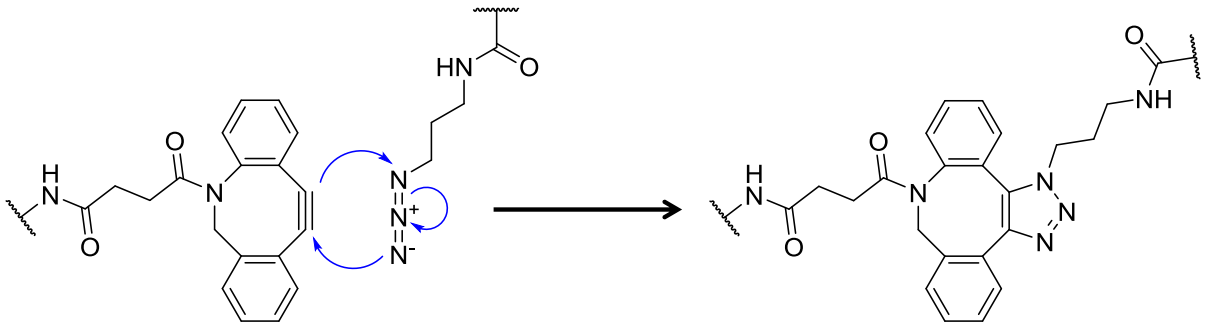

Figure 26. Mechanism for the cyclization of a strained cyclooctyne and azide biorthogonal pair.

With this in mind, we next assessed whether MASML was compatible with a representative bioorthogonal ligation system. To this end we explored the MASML using sDARP and a nucleophile tethered to a strained cyclooctyne (GGK^{DBCO}). Similar to the reactions described above, The C-terminal modification of sDARP with GGK^{DBCO} was performed in the presence or absence of Ni^{2+} and monitored by ESI-MS for 9 hours (**Figure 27a**). The (-)Ni^{2+} reaction reached completion at 5 hours and achieved a maximum conversion of 38%, while the (+)Ni^{2+} reaction was much more successful, reaching a conversion of 85% at the 9hr timepoint, (**Figure 27b**). Hydrolysis was observed to increase for the (+)Ni^{2+} reactions, with a modest increase from <0.5% to 3.5% with the addition of Ni^{2+}.

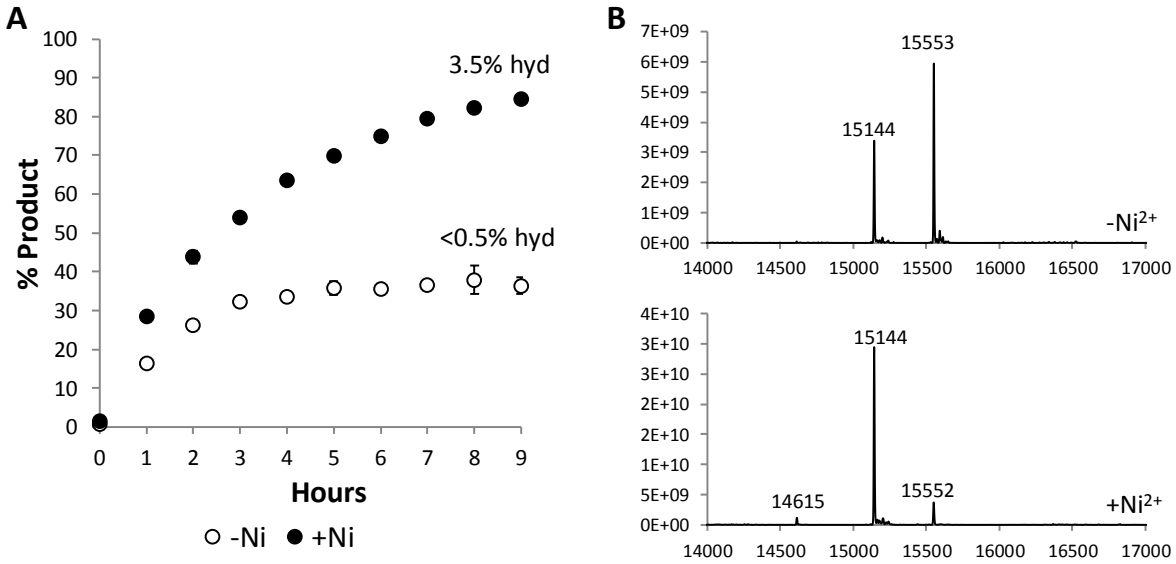

Figure 27. ESI-MS data for the C-terminal modification of sDARP with GGK^{DBCO}. (**A**) Product conversion for both reactions was estimated by ESI-MS. All data points represent the averaged of two trials, with error bars corresponding to the full range of the data set. (**B**) ESI-MS spectra from the 9hr timepoints of the $(+)Ni^{2+}$ (bottom) and $(-)Ni^{2+}$ (top) reactions (calculated molecular weights: sDARPin = 15550 Da, sDARP(DBCO) = 15142 Da, hydrolyzed sDARP = 14613 Da).

We next evaluated whether the ligation product from the MASML reaction could participate in a strain-promoted cycloaddition with a suitable azide reagent. Ultimately, a one pot reaction sequence was developed that first involved the installation of DBCO followed by a strain-promoted click reaction (**Figure 28**). As shown in **Figure 28**, a MASML reaction between sDARP and one equivalent of GGK^{DBCO} was performed in the presence of Ni^{2+} as described above. After a 9 hour room temperature incubation, the MASML reaction gave conversion to the DBCO conjugated product (78.5%, estimated by ESI-MS). Two equivalents of azido 6-FAM were then added to the crude reaction mixture, and the click reaction was tracked via ESI-MS. After 15min, the reactions saw a 63.5% yield of the secondary ligation product ($sDARP(6\text{-}FAM)_{click}$), which corresponds to an 80.0% consumption of the original ligation product, sDAPR(DBCO). The reaction reached completion by 45min with a final product amount of 73.7% relative to the original,

unmodified DARPin substrate. This was equal to a 91.9% conversion of the original ligation product.

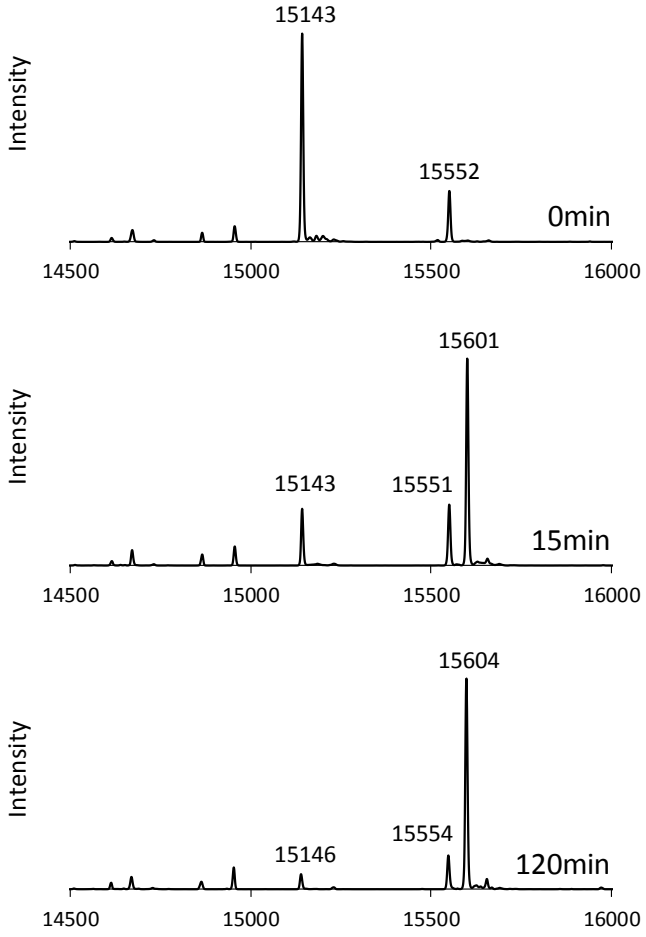

Figure 28. ESI-MS data for the secondary ligation of sDARP with azido 6-FAM. (Top) Reconstructed spectra of the reaction mixture after 9hrs of ligation, before addition of azido 6-FAM. (Middle) Spectra from 15min after the addition of azido 6-FAM. (Bottom) Spectra from 2hrs after the addition of azido 6-FAM. (Expected masses: sDARP = 15550 Da, sDARP(DBCO) = 15143 Da, sDARP(6-FAM)$_{click}$ = 15599 Da).

Given the high initial yield of DBCO-functionalized sDARP, and the near complete conversion to the secondary click product, the one-pot experiment setup proved successful. At this point, a simple affinity purification scheme could be applied to remove unmodified sDARP still possessing the C-terminal His$_6$-tag. While some unreacted

sDARP(DBCO) would still remain, the final mixture would contain a greater than 90% purity of sDARP(6-FAM)$_{click}$.

4. Conclusions and Future Directions

The data in this thesis illustrate the significant enhancement provided by the addition of nickel to sortase-mediated ligation reactions and demonstrate a broader range of protein-based MASML applications than has been shown. Previously, high yields from SML strategies were only achievable through the use of excess reagent or by significantly altering the reagents and ligation site used for the sortase-mediated ligation. This work, in conjunction with previous studies from the Antos group, shows that MASML is an excellent alternative. MASML is compatible with a variety of protein targets (many of which are in development as therapeutics), allows for a wide range of modifications, and requires only the use of a simple solution additive (Ni^{2+}) to improve ligation efficiency.

This work has a number of implications for the continued development of sortase-based methods for protein engineering. For instance, we have shown SrtA possesses variable reagent affinity, even when the nucleophile base peptides or substrate C-termini are similar. Given SML reactions are typically performed under conditions of excess reagent, these trends of selectivity are not often apparent, but are obvious when neither reagent is limiting. The ligation of sDARP and Cy3, for example, gave impressive yields even in the absence of nickel, while reactions using the DBCO and 6-FAM appended nucleophiles saw a doubling of yields with the addition of nickel (**Figure 29**). Interestingly, we have shown that while some reagent-specificity is present when working at equimolar concentrations, the enzyme's selectivity is effectively eliminated with the use of MASML,

with yields improved for all reactions (except those involving sAff) to greater than 80%, even for those with low yields in the absence of Ni^{2+} (**Figure 29**).

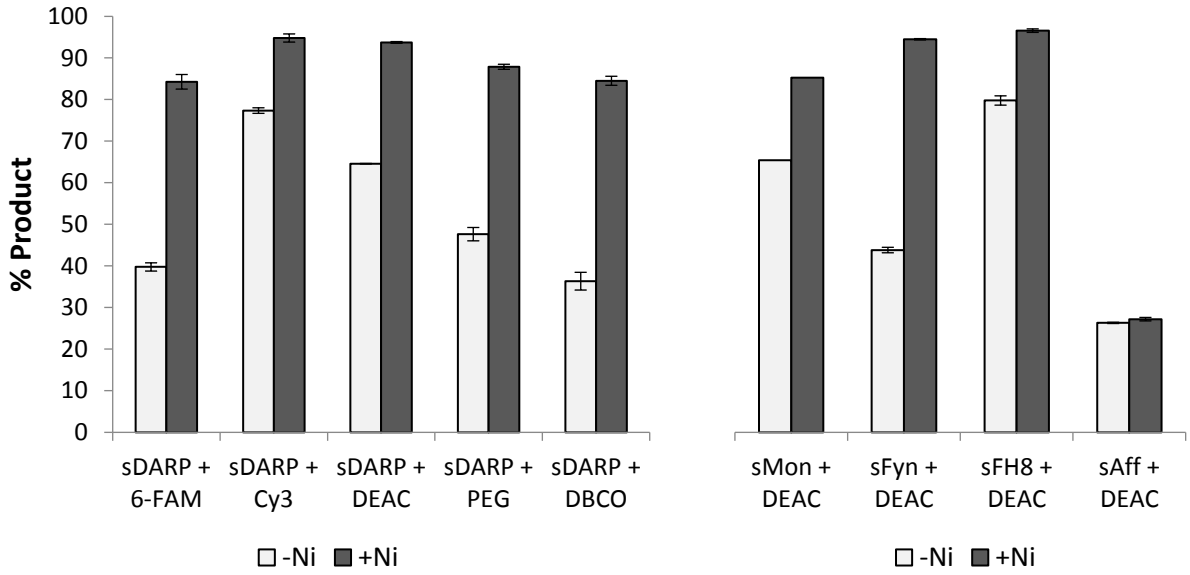

Figure 29. Final yields for all ligation pairings, with (-)Ni^{2+} reactions shown in light gray, and (+)Ni^{2+} shown in dark gray. Each bar represents the mean of two trials (except for the sMon reaction), with error bars corresponding to the full range of the data set.

In addition, this work effectively demonstrates the compatibility of MASML with the modification of antibody-alternative scaffolds, using the same sortase-ready C-terminal sequence which has been used in previous studies involving the modification of antibodies. The $LPXTGGH_6$ sequence is a common motif in sortase-catalyzed ligations, a recent example being the generation of antibody drug conjugates using SML to replicate commercial conjugates, which were shown to have identical *in vitro* activity.[27] SML has also been applied to the fluorescent labeling of antibodies, as well as the generation of crosslinked antibody-derived constructs to aide in overcoming the antibody resistance of HIV-1.[24] The data presented in this thesis demonstrate the effective improvement in conjugate yields achievable with MASML in the context of antibody mimetics but can in

theory be applied to antibodies as well. Sortase-ready antibodies have already been established in previous literature, and so the application of this technique to those systems would involve the simple addition of a cheap reagent, $NiSO_4$, with no additional alterations required for either the antibody substrates or the glycine nucleophile-associated modifications.

Furthermore, with a growing interest in molecules such as monobody, affibody, and fynomer as smaller alternatives to full-sized antibodies, the ability to adapt established SML methods for the generation of ADCs for use on non-antibody molecules, is a promising direction for future studies. We have also shown while optimization may be necessary, as was the case with monobody, even a slight excess of nickel in the reaction mixture was sufficient to increase yields, showing the tolerance of this method to adjustments for specific reagents and conditions.

Overall, this research also provides a basis for future MASML work in the context of N-terminal modifications, as well as protein-protein ligations. The same protein targets can be used as nucleophiles if modified to contain N-terminal glycines, and the panel of modifications can be appended to synthetic substrates in a similar manner as the addition to synthetic nucleophiles. Showing the applicability of MASML to these types of reactions would help to provide a more complete foundation for enhancing future sortase-based syntheses.

5. Experimental

5.1 Protein Expression and Purification

Sequences of proteins used in this study:

SrtA$_{Staph}$
MRGSSHHHHHHSSGLVPRGSHMQAKPQIPKDKSKVAGYIEIPDADIKEPVYPGPATPE
QLNRGVSFAEENESLDDQNISIAGHTFIDRPNYQFTNLKAAKKGSMVYFKVGNETRKY
KMTSIRDVKPTDVGVLDEQKGKDKQLTLITCDDYNEKTGVWEKRKIFVATEVK

sDARP
MRGDLGKKLLEAARAGQDDEVRILMANGADVNAKDEYGLTPLYLATAHGHLEIVEVLL
KNGADVNAVDAIGFTPLHLAAFIGHLEIAEVLLKHGADVNAQDKFGKTAFDISIGNGNED
LAEILQKLNGGGGSGGGGSLPETGGHHHHHH

sAff (*initiator methionine absent in purified protein*)
VDNKFNKEMRNAYWEIALLPNLNNQQKRAFIRSLYDDPSQSANLLAEAKKLNDAQAPK
GGGGSGGGGSLPETGGHHHHHH

sMon
MRGSSVSSVPTKLEVVAATPTSLLISWDAPMSSSSVYYYRITYGETGGNSPVQEFTVP
YSSSTATISGLSPGVDYTITVYAWGEDSAGYMFMYSPISINYRTGGGGSGGGGSLPET
GGHHHHHH

sFyn
MRGSGVTLFVALYDYQADRWTDLSFHKGEKFQILDASPPGDWWEARSLTTGETGYIP
SNYVAPVDSIQGEQKLISEEDLGGGGSGGGGSLPETGGHHHHHH

sFh8 (*initiator methionine absent in purified protein*)
PSVQEVEKLLHVLDRNGDGKVSAEELKAFADDSKCPLDSNKIKAFIKEHDKNKDGKLDL
KELVSILSSGTSENLYFQGEEKKENDKEEGSMSSRIESLTIQEDAKEGVEDEEDGGGG
SGGGGSLPETGGHHHHHH

Plasmid Preparation. The pET-28a vector encoding SrtA$_{Staph}$ was obtained from the Addgene plasmid repository (plasmid #51138). Expression vectors for sDARP, sMon, sFyn, sAff, and sFh8 were obtained by commercial gene synthesis from ATUM, and were prepared in the pD441-SR plasmid backbone.

Expression and purification of substrate proteins. All protein substrates were generated using the same general expression and purification scheme. Plasmids containing the desired protein were transformed into BL21(DE3) chemically competent *E. coli* cells via heat shock, and the cells were then plated onto LB-agar plates containing 100 µg/mL kanamycin. The plates were incubated at 37°C overnight. Single colonies were collected from the plates and used to inoculate 50mL of LB broth containing kanamycin at 100 µg/mL. These seed cultures were incubated with shaking at 37°C for approximately 18 hours. The full 50mL starter cultures were then added to 1L of sterile LB broth containing 100 µg/mL kanamycin and incubated at 37°C with shaking. The 1L growths were incubated until an OD_{600} of 0.8-0.9 was reached, at which point IPTG was added (1mM final concentration) to induce protein expression. The cultures were then incubated at 37°C with shaking for 3 hours. The cells were harvested by centrifugation at 4,629xg for 10min.

Cell pellets were stored at -80°C until purification, at which point they were thawed on ice in 30mL of lysis buffer (20mM Tris (pH 7.5), 150mM NaCl, 0.5mM EDTA). Once thawed, lysozyme was added to a final concentration of 10 mg/mL and the cell suspensions were shaken at room temperature for 1 hour. The resuspended cells were sonicated twice, for 30 second intervals at 50% output. The lysate was clarified by centrifugation at 39,375xg for 30min. The protein-containing supernatant was added to 5mL of His-Bind (Thermo-Fisher) Ni-NTA resin equilibrated in wash buffer (20mM Tris (pH 7.5), 150mM NaCl, 20mM imidazole). The column was then flushed with 10 column volumes of wash buffer. The remaining bound protein was eluted using 10mL of elution

buffer (20mM Tris (pH 7.5), 150mM NaCl, 300mM imidazole), collected as two 5mL fractions.

The gravity flow IMAC purified fractions were desalted using a 10mL Bio-Scale Mini Bio-Gel desalting cartridge (Bio-Rad) on an NGC Quest 10 Plus FPLC system (Bio-Rad) to remove imidazole. Desalting was achieved following the manufacturer's protocol using a mobile phase buffer consisting of 20mM Tris (pH 7.5) and 150mM NaCl at a flow rate of 2 mL/min. The desalted proteins were then analyzed via ESI-MS to confirm protein identity and to assess purity. In general, minor impurities were detected in most of the gravity-flow purified protein stocks. To remove these impurities, a second IMAC purification was performed using a 5mL Bio-Scale Mini IMAC affinity cartridge (Bio-Rad) on an NGC Quest 10 Plus FPLC system (Bio-Rad). Briefly, the IMAC cartridge was first equilibrated with 20mM Tris (pH 7.5), 150mM NaCl, and 20mM imidazole. Proteins were then loaded onto the IMAC cartridge at a flow rate of 7 mL/min. A gradient elution of 20-300 mM imidazole was then used to elute the target proteins (flow rate = 7 mL/min). Fractions were then examined by ESI-MS and pure fractions were combined, then desalted using the same desalting technique described previously (**Appendix III**). The final storage buffer for all proteins consisted of 20mM Tris (pH 7.5) and 150mM NaCl. Protein stocks were also analyzed by SDS-PAGE to confirm purity (**Appendix III**).

Determination of protein concentration. All protein concentrations were determined using a Nanodrop^{TM} ND-1000 spectrophotometer (Thermo Scientific) at 280nm. The molar extinction coefficients used were 2980 cm^{-1} M^{-1} for sDARP, 8480 cm^{-1} M^{-1} for sAff, 1490 cm^{-1} M^{-1} for sFh8, 22460 cm^{-1} M^{-1} for sFyn, and 25900 cm^{-1} M^{-1} for sMon. Extinction

coefficients were estimated from the individual protein sequences using ExPASy ProtParam.

5.2 Peptide Synthesis

All reagents were acquired from the indicated commercial sources and used without additional purification. HPLC purification and analysis were performed on a Dionex Ultimate 3000 HPLC system (Thermo Scientific). ESI-MS was performed on an expression^{L} CMS (Advion) attached to the above HPLC system. Analytical scale peptide analyses were performed on a Kinetex® 2.6µm, C18 100Å LC column (100 x 2.1mm) (C18, Phenomenex®) using the following method (Method A): H_2O (5% acetonitrile, 0.1% formic acid)/organic (MeCN, 0.1% formic acid) mobile phase. Flow rate = 0.4 mL/min. Gradient = 5% organic (0.0-1.0 min), 5% organic to 90% organic (1.0-7.0 min), hold 90% organic (7.0-9.0 min), 90% organic to 5% organic (9.0-9.1 min), equilibrate back to 5% organic (9.1-12.0 min).

Peptides were purified on a Luna 5u, C18(2) 100Å column (250 x 10mm) (semi-prep, Phenomenex®) using one of the following methods: (Method B): H_2O (5% acetonitrile, 0.1% formic acid)/organic (MeCN, 0.1% formic acid) mobile phase. Flow rate = 4 mL/min. Gradient = 10% organic (0.0-2.0 min), 10% organic to 90% organic (2.0-12.0 min), hold 90% organic (12.0-14.0 min), 90% organic to 10% organic (14.0-14.1 min), equilibrate back to 10% organic (14.1-17.0 min). (Method C): H_2O (5% acetonitrile, 0.1% TFA)/organic (MeCN, 0.1% TFA) mobile phase. Flow rate = 4 mL/min. Gradient = 20% organic (0.0-2.0 min), 20% organic to 90% organic (2.0-15.0 min), hold 90% organic (15.0-17.0 min), 90% organic to 20% organic (17.0-17.1 min), equilibrate back to 20%

organic (17.1-19.0 min). (Method D): H_2O (5% acetonitrile, 0.1% TFA)/organic (MeCN, 0.1% TFA) mobile phase. Flow rate = 4 mL/min. Gradient = 20% organic (0.0-2.0 min), 20% organic to 70% organic (2.0-15.0 min), 70% organic to 90% organic (15.0-15.1 min), hold 90% organic (15.1-17.0 min), 90% organic to 10% organic (17.0-17.1 min), equilibrate back to 20% organic (17.1-19.0 min).

Solid-phase peptide synthesis. The base peptides (Fmoc-GGK and Fmoc-GGKY) for all nucleophiles was synthesized on a 0.2mmol scale using rink amine MBHA resin (AnaSpec Inc.). The resin was first washed/swollen in NMP. Deprotection was then performed by treatment with 20% piperidine in NMP (10mL, 2x, 10min each) followed by washes with pure NMP (10mL, 3x, 5min each) to remove cleaved Fmoc. The deprotected resin was then treated with a coupling mixture containing an Fmoc-protected amino acid (Chem-Impex Int'l Inc., 0.6mmol), HBTU (Chem-Impex Int'l Inc., 0.6mmol) and DIPEA (1mM) solvated in ~3mL of NMP. Coupling occurred at room temperature with shaking for 1 hour or overnight. Unreacted components were washed from the resin mixture using NMP (10mL, 3x, 5min each). Additional amino acids were added using the same method of deprotection, washing, and coupling.

The base peptides were not subjected to Fmoc deprotection before cleavage from the resin, so as to leave only one nucleophilic amine for later modification. Cleavage was achieved by first washing the resin with DCM (10mL, 3x, 5min each), then incubating with cleavage solution (95/2.5/2.5 TFA/ddH_2O/TIPS) for 30min (2x, 5 mL each). After each incubation period, the cleavage solution was drained and collected. TFA was removed via rotary evaporation. The remaining peptide solution was precipitated by drop-wise addition to dry ice-chilled diethyl ether. The precipitated peptides were then pelleted by

centrifugation at 4,696xg for 5min. Supernatant was removed, and pelleted peptides were dried under vacuum overnight. The crude peptides were then resolubilized in NMP to a final concentration of approximately 100 mg/mL.

Modification of base-peptide with desired functional group. Once the base peptides had been generated, they were used without further purification to generate the nucleophile library used in this thesis. Modifications were installed via reaction of the base peptides (Fmoc-GGK or Fmoc-GGKY) with activated ester derivatives of the desired modifications. Ligation mixtures were prepared on a scale to yield 3mg of the end product (15mg, in the case of $GGK^{dPEG2000}Y$) using a 2x molar excess of the base peptide relative to the activated ester. The base peptide for all nucleophiles was Fmoc-GGK, except in the case of $GGK^{dPEG2000}Y$, which was generated using Fmoc-GGKY for quantification purposes as PEG does not have a unique absorbance maximum. The ligation process was tracked by HPLC and ESI-MS using a C18 column and Method A. When no more unligated modification could be detected, piperidine was added to a final concentration of 20% (v/v) to remove the N-terminal Fmoc group. The reaction was again observed using HPLC and ESI-MS (Method A) until deprotection was complete (see **Appendix I** for example spectra).

Synthesis of $GGK^{6\text{-}FAM}$. Fmoc-GGK (9.72 µmol), NHS-6-FAM (AnaSpec**,** 4.86µmol), and DIPEA (29.2µmol) were combined in NMP (100µL total volume). The reaction was complete after 30 min as determined by ESI-MS (expected mass for Fmoc-$GGK^{6\text{-}FAM}$ $[M+H]^+$ = 840.3 Da, observed mass = 840.3 Da). Piperdine (25µL, 20% v/v) was then added to remove the Fmoc group. Deprotection was monitored by ESI-MS, and

determined to be complete by 30 min (expected mass for $GGK^{6\text{-}FAM}$ $[M+H]^+$ = 618.2 Da, observed mass = 618.3 Da).

Synthesis of GGK^{Cy3}. Fmoc-GGK (8.58μmol), NHS-Cy3 (Lumiprobe, 4.29μmol), and DIPEA (25.7μmol) were combined in NMP (100μL total volume). The reaction was complete after 60 min as determined by ESI-MS (expected mass for Fmoc-GGK^{Cy3} $[M+H]^+$ = 921.5 Da, observed mass = 921.8 Da). Piperdine (25 μL, 20% v/v) was then added to remove the Fmoc group. Deprotection was monitored by ESI-MS, and determined to be complete by 30 min (expected mass for GGK^{Cy3} $[M+H]^+$ = 698.9 Da, observed mass = 698.7 Da).

Synthesis of GGK^{DEAC}. Fmoc-GGK (11.9μmol), NHS-DEAC (Sigma Life Science, 5.97μmol), and DIPEA (35.82μmol) were combined in NMP (100μL total volume). The reaction was complete after 90 min as determined by ESI-MS (expected mass for Fmoc-GGK^{DEAC} $[M+H]^+$ = 725.3 Da, observed mass = 725.3 Da). Piperidine (25 μL, 20% v/v) was then added to remove the Fmoc group. Deprotection was monitored by ESI-MS, and determined to be complete by 90 min (expected mass for GGK^{DEAC} $[M+H]^+$ = 503.3 Da, observed mass = 503.3 Da).

Synthesis of GGK^{DBCO}. Fmoc-GGK (11.0μmol), NHS-DBCO (Conju-Probe, 5.49μmol), and DIPEA (32.9μmol) were combined in NMP (100μL total volume). The reaction was complete after 25 min as determined by ESI-MS (expected mass for Fmoc-GGK^{DBCO} $[M+H]^+$ = 769.3 Da, observed mass = 769.3 Da). Piperidine (25 μL, 20% v/v) was then added to remove the Fmoc group. Deprotection was monitored by ESI-MS, and determined to be complete by 50 min (expected mass for GGK^{DBCO} $[M+H]^+$ = 547.3 Da, observed mass = 547.3 Da).

Synthesis of GGK^{dPEG2000}Y. Fmoc-GGKY (10.7 µmol), TFP-dPEG2000 (Quanta Biodesign Lmt., 5.33 µmol), and DIPEA (32.0 µmol) were combined in NMP (100 µL total volume) and analyzed via ESI-MS every 15 min. The expected $[M+2H]^{2+}$ for Fmoc-GGK^{dPEG2000}Y was 1409.3 Da, and the observed mass was 1409.7 Da. The ligation reached completion at 90min, at which point piperidine (25µL, 20% v/v) was added to remove the Fmoc group. Deprotection was complete by 60min as determined by ESI-MS. The expected molecular weight for GGK^{dPEG2000}Y was 2594.4 Da and was observed as $[M+3H]^{3+}$ (expected: 866.4 Da, observed: 866.3 Da) and as a number of ammonium adducts: $[M+1H+2NH_4]^{3+}$ (expected: 877.7 Da, observed: 877.6 Da), $[M+2H+NH_4]^{3+}$ (epected: 872.0 Da, observed: 871.9 Da), $[M+2H+2NH_4]^{4+}$ (expected: 658.5 Da, observed: 658.5 Da), $[M+3H+NH_4]^{4+}$ (expected: 654.3 Da, observed: 654.4 Da).

Nucleophile Purification. All peptide nucleophiles were purified by HPLC prior to use in sortase-mediated ligation reactions. Product peaks were tracked at the λ_{max} for the respective functional groups, and separations were achieved using a semi-prep column with HPLC Methods B, C, or D (**Table 1**). Pure fractions were pooled and MeCN and formic acid were removed from the purified peptide solution by rotary evaporation. The remaining peptide solution was frozen over dry-ice and lyophilized. Dry peptides were resolubilized in DMSO, water, or a mixture of both depending on the solubility of the modification (**Table 1**). Final stock concentrations were determined using a Nanodrop^{TM} ND-1000 spectrophotometer (Thermo Scientific) at the λ_{max} for the modification and using the appropriate molar extinction coefficients listed below in **Table 1**. For most applications, stocks were diluted to approximately 1mM for use in reactions and underwent final ESI-MS and UV-Vis analysis to confirm identity and purity (**Appendix II**).

Table 1. Purification and quantification parameters for the nucleophile library.

Modification	λ_{max}	Molar Extinction Coefficient (M^{-1} cm^{-1})	Purification Method	Final Solvent Composition
6-FAM	495 nm	75,000	D	DMSO
Cy-3	555 nm	150,000	C	DMSO
DEAC	429 nm	46,800	B	5:2 ddH_2O:DMSO
DBCO	309 nm	12,000	B	5:1 ddH_2O:DMSO
dPEG2000*	280 nm	1,280	B	ddH_2O

*(quantified using the Tyr present in base peptide)

5.3 General procedure for Sortase Catalyzed Ligations

Analytical scale separations of full-sized proteins for ESI-MS were performed using an Aeris™ 3.6µm, WIDEPORE C4 200Å LC column (100 x 2.1mm) (C4, Phenomenex®). LC-ESI-MS analyses performed on the C4 used the following method (Method E): H_2O (5% acetonitrile, 0.1% formic acid) / organic (MeCN, 0.1% formic acid) mobile phase. Flow rate = 0.3 mL/min. Gradient = 10% organic (0.0-0.5 min), 10% organic to 90% organic (0.5-7.0 min), hold 90% organic (7.0-8.0 min), 90% organic to 10% organic (8.0-8.1 min), equilibrate back to 10% organic (8.1-13.25 min).

All C-terminal SML and MASML reactions, with the exception of the ligation of sMon and GGK^{DEAC}, performed for this thesis used the same basic reaction composition listed in **Table 2** and were performed at room temperature unless otherwise indicated**.** Reactions were run on 100µL scale, and all reactions also contained 10% (v/v) 10x sortase reaction buffer (500mM Tris (pH 7.5), 1.5M NaCl, and 100mM $CaCl_2$). Reactions were analyzed every hour via ESI-MS, using the C4 column and HPLC Method E. The mass range used was 500-1800 Da. Raw ESI-MS data from each timepoint was processed using the following three-step protocol: the raw chromatogram data was first exported from Advion Data Expression (Ver 3.0) as .CDF files, and reconstructed in

MNova (Ver 10.0). The mass peak corresponding to the unmodified substrate and ligation product was highlighted and the spectra extracted. These spectra were converted to text files and opened in Analyst® (Ver 1.4) to reconstruct the mass graph (maximum entropy algorithm). Product conversion was then calculated using area-under-the-curve for the starting material, ligation product, and hydrolysis product. This was performed at each timepoint and averaged across duplicate trials.

Table 2. Reaction concentrations of each reagent in the C-terminal SML/MASML reactions (using equimolar amounts of substrate and nucleophile) completed in this study.

Reagent	(+)Ni^{2+}	(-)Ni^{2+}
Substrate	50 µM	50 µM
Nucleophile	50 µM	50 µM
$NiSO_4$ (Ni^{2+})	200 µM	0 µM
$SrtA_{Staph}$	10 µM	10 µM

The SML/MASML of sMon and GGK^{DEAC} was adjusted to account for the insolubility of monobody is the presence of excess Ni^{2+} (**Table 3**). As in the case of other targets, sMon reactions were run on 100µL scale, and all reactions contained 10% (v/v) 10x sortase reaction buffer (500mM Tris (pH 7.5), 1.5M NaCl, and 100mM $CaCl_2$). The reactions were allowed to proceed at room temperature, with 20µL aliquots collected at 0, 6, 12, and 24hrs. These samples were quenched using 6.67µL of a 4X DTT-containing SDS-PAGE loading buffer, and a second 24hr aliquot was quenched with an equal volume of MeCN (0.1% formic acid). The loading buffer-quenched samples were analyzed by SDS-PAGE (10µL loading volume). ESI-MS analysis was performed on the MeCN quenched 24hr samples, using HPLC Method E and a 500-1800 Da mass range.

Table 3. Reaction concentrations of each reagent in the C-terminal modification of sMon with GGK^{DEAC}.

Reagent	(+)Ni^{2+}/ (+)DMSO	(-)Ni^{2+}/ (+)DMSO	(-)Ni^{2+}/ (-)DMSO
Substrate	50 µM	50 µM	50 µM
Nucleophile	50 µM	50 µM	50 µM
$NiSO_4$ (Ni^{2+})	100 µM	0 µM	0 µM
DMSO	20%	20%	0%
$SrtA_{Staph}$	10 µM	10 µM	10 µM

Optimization of sDARP and GGK^{DEAC} ligation reaction. These reactions were run in duplicate and analyzed via the method outlined above. sDARP (50µM) was combined with varying amounts of GGK^{DEAC}: 1x (50µM), 2x (100µM), 3x (150µM), 5x (250µM), or 20x (1mM) in the absence of Ni^{2+} additive. Each reaction was run in duplicate on 100 µL scale and analyzed by ESI-MS. All reactions contained 10% (v/v) 10x sortase reaction buffer (500mM Tris (pH 7.5), 1.5M NaCl, and 100mM $CaCl_2$).

Combined MASML and Bioorthogonal Ligation Reaction. sDARP (50µM) was combined with GGK^{DBCO} (50µM) and $SrtA_{Staph}$ (10µM) in the presence or absence of Ni^{2+} (from $NiSO_4$, 200µM). The reaction was performed on a 100 µL scale and contained 10% (v/v) 10x sortase reaction buffer (500mM Tris (pH 7.5), 1.5M NaCl, and 100mM $CaCl_2$). The reaction mixture was examined after 9 hours by ESI-MS. After the initial 9hr ligation period, azido 6-FAM was directly added to the reaction mixture (1.09 µL of a 450 µM DMSO stock solution, 100µM final concentration of azido 6-FAM). The biorthogonal ligation reaction was then monitored by ESI-MS every 15 min, over the course of 2 hours.

6. Literature Cited

1. Carter, P. Site-directed mutagenesis. *Biochem J.* **1986**, *237*: 1-7.
2. Könning, D. and Kolmar, H. Beyond antibody engineering: directed evolution of alternative binding scaffolds and enzymes using yeast surface display. *Micro Cell Fact.* **2018**, *17*(32).
3. Caucheteur, D; Robin, G.; Parez, V.; Martineau, P. Construction of a synthetic antibody gene library for the selection of intrabodies and antibodies. *Methods Mol Biol.* **2017**, *1701*: 239-253.
4. Park, S. H.; Uzawa, T.; Hattori, F.; Ogino, S.; Morimoto, N.; Tsuneda, S.; Ito, Y. “All-in-one” in vitro selection of collagen-binding vascular endothelial growth factor. *Biomaterials*. **2018**, *161*: 270-278.
5. Noren, C. J.; Anthony-Cahill, S. J.; Griffith, M. C.; Schultz, P. G. *Science*. **1989**, *244*: 182-188.
6. Lee, T. C.; Kang, M.; Kim, C. H.; Schultz, P. G.; Chapman, E.; Deniz, A. A. Dual unnatural amino acid incorporation and click-chemistry labeling to enable single-molecule fret studies of p97 folding. *ChemBioChem*. **2016**, *17*: 981-984.
7. Lang, K. and Chin, J. W. (2014) Cellular incorporation of unnatural amino acids and bioorthogonal labeling of proteins. *Chem Rev.* **2014**, *114*: 4764-4806.
8. Wals, K and Ovaa, H. Unnatural amino acid incorporation in E.coli: current and future applications in the design of therapeutic proteins. *Front Chem*. **2014,** *2*(15).
9. Metildi, C. A.; Kayshal, S.; Luiken, G. A; Talamini, M. A.; Hoffman, R. M.; Bouvet, M. (2014) Fluorescently labeled chimeric anti-cea antibody improves detection and

resection of human colon cancer in a patient-derived orthotopic xenograft (PDOX) nude mouse model. *J Surg Oncol*. **2014**, *109*: 451-458.

10. de Bruin, B.; Kuhnast, B.; Hinnen, F.; Yaouancq, L.; Amessou, M.; Johannes, L.; Samson, A.; Boisgard, R.; Tavitian, B.; Dollé. F. 1-[3-(2-[18F]Fluoropyridin-3-yloxy)propyl]pyrrole-2,5-dione: design, synthesis, and radiosynthesis of a new [18F]Fluoropyridine-based maleimide reagent for the labeling of peptides and proteins. *Bioconjugate Chem*. **2005**, *16*: 406-420.
11. Ducry, L. and Stump, B. Antibody-drug conjugates: linking cytotoxic payloads to monoclonal antibodies. *Bionconjugate Chem.* **2010**, *21*: 5-13.
12. Jevševar, S.; Kunstelj, M.; Porekar, V. G. PEGylation of therapeutic proteins. *Biotechnol J*. **2010**, *5*: 113–128.
13. Dozier, J. K. and Distefano, M. D. Site-specific PEGylation of therapeutic proteins. *Int J Mol Sci*. **2015**, *16*: 25831–25864.
14. Baslé, E.; Joubert, N.; Pucheault, M. Protein chemical modification on endogenous amino acids. *Chemistry & Biology*. **2010**, *17*: 213-227.
15. Rabuka, D. Chemoenzymatic methods for site-specific protein modification. *Current Opinion in Chemical Biology*. **2012**, *14*: 790-796.
16. Payne, J. T.; Poor, C. B.; Lewis, J. C. Directed evolution of RebH for site-specific halogenation of large biologically active molecules. *Angew Chem Int Ed*. **2015**, *54*: 1-6.
17. Kan, S. B. J.; Lewis, R. D.; Chem, K.; Arnold, F. H. Directed evolution of cytochrome c for carbon-silicon bond formation: bringing silicon to life. *Science*. **2016**, *354*(6315): 1048-1051.

18. Li, Z.; Theile, C. S.; Chen, G. Y.; Bilate, A. M.; Durate, J. N.; Avalos, A. M.; Fang, T.; Barberena, R.; Sato, S.; Ploegh, H. L. Fluorophore-conjugates Holliday Junctions for generating super-bright antibodies and antibody fragments. *Angew Chem Int Ed*. **2015**, *54*: 11706-11710.

19. Shi, J.; Kundrat, L.; Pishesha, N.; Bilate, A.; Theile, C.; Maruyama, T.; Dougan, S. K.; Ploegh, H. L.; Lodish, H. F. Engineered red blood cells as carried for systemic delivery of a wide array of functional probes. *PNAS*. **2014**, *111*(28): 10131-10136.

20. Park, K.; Jung, J.; Son, J.; Kim, S. H.; Chung, B. H. Anchoring foreign substances on live cell surfaces using sortase A specific binding peptide. *Chem Commun*. **2013**, *49*: 9585-9587.

21. Pasqual, G.; Chudnovsky, A.; Tas, J. M. J.; Agudelo, M.; Schweitzer, L. D.; Cui, A.; Hacohen, N.; Victora, G. D. Monitoring T cell-dendritic cell interactions *in vivo* by intercellular enzymatic labelling. *Nature*. **2018**. *553*: 496-500.

22. Pierce, N. W.; Lee, J. E.; Liu, X.; Sweredoski, M. J.; Graham, R. L. J.; Larimore, E. A.; Rome, M.; Zheng, N.; Clurman, B. E.; Hess, S.; Shan, S.; Deshaies, R. J. Cand1 promotes assembly of new SCF complexes through dynamic exchange of F Box proteins. *Cell*. **2013**, *153*: 206-215.

23. Guimaraes, C. P.; Witte, M. D.; Theile, C. S.; Bozkurt, G.; Kundrat, L.; Blom, A. E. M.; Ploegh, H. L. Site-specific C-terminal and internal loop labeling of proteins using sortase-mediated reactions. *Nature Protocols*. **2013**, *8*: 1787-1799.

24. Galimidi, R. P.; Klein, J. S.; Politzer, M. S.; Bai, S.; Seaman, M. S.; Nussenzweig, A. P. W.; Bjorkman, P. J. Intra-spike crosslinking overcomes antibody evasion by HIV-1. *Cell*. **2015**, *160*: 433-446.

25. Krueger, A. T.; Kroll, C.; Sanchez.; Griffith, L. G.; Imeriali, B. tailoring chimeric ligands for studying and biasing ErbB receptor family interactions. *Angew Chem Int Ed Engl.* **2014**, *53*(10): 2662-2666.

26. Xu, Y.; Jin, S.; Zhao, W.; Liu, W.; Ding, D.; Zhou, J.; Chen, S. A versatile chemo-enzymatic conjugation approach yields homogenous and highly potent antibody-drug conjugates. *Int J Mol Sci*. **2017**, *18*(2248).

27. Beerli, R. R.; Hell, T.; Merkel, A. S.; Grawunder, U. Sortase enzyme-mediated generation of site-specifically conjugates antibody drug conjugates with high *in vitro* and *in vivo* potency. *PLoS*. **2015**, *10*(7).

28. Carrico, I. S.; Carlson, B. L.; Bertozzi, C. R. Introducing genetically encoded aldehydes into proteins. *Nature Chem Bio*. **2007**, *3*(6): 321-322.

29. Wakabayashi, R; Yahiro, K.; Hayashi, K.; Goto, M.; Kamiya, N. Protein-grafted polymers prepared through a site-specific conjugation by microbial transglutaminase for an immunosorbent assay. *Biomacromolecules*. **2017**, *18*(2): 422-430.

30. Ritchie, C.; Cylinder, I.; Platt, E. J.; Barklis, E. Analysis of HIV-1 gag protein interactions via biotin ligase tagging. *J Virol*. **2015**, *89*(7): 3988-4001.

31. Best, M.; Degen, A.; Baalmann, M.; Schmidt, T. T.; Wombacher, R. Two-step protein labeling using norbornene substrates for lipoic acid ligase and the inverse-electron demand diels-alder reaction. *ChemBioChem*. **2015**, *16*(8): 1158-1162.

32. Antos, J. M.; Truttmann, M. C.; Ploegh, H. L. Recent advances in sortase-catalyzed ligation methodology. *Curr Opin Struct Biol.* **2016**, *38*: 111-118.

33. Comfort, D. and CLubb, R. T. A comparative genome analysis identifies distinct sorting pathways in gram-positive bacteria. *Infect Immun*. **2004**, *72*(5): 2710-2722.

34. Mao, H.; Hart, S. S.; Schink, A.; Pollok, B. A. Sortase-mediated protein ligation: a new method for protein engineering. *J Am Chem Soc*. **2004**, *126*: 2670-2671.

35. Mazmanian, S. K.; Liu, G.; Ton-That, H.; Schneewing, O. *Staphylococcus aureus* sortase, an enzyme that anchors surface proteins to the cell wall. *Science*. **1999**, *285*: 760-763.

36. Spirig, T.; Weiner, E. M.; Clubb, R. T. Sortase enzymes in gram-positive bacteria. *Mol Microbiol.* **2011**, *82*(5): 1044-1059.

37. Maresso, A. W.; Chapa, T. J.; Schneewind, O. Surface protein IsdC and sortase B are required for heme-iron scavenging of *Bacillus anthracis*. *J Bacteriol*. **2006**, *188*(23): 8145-8152.

38. Kang, H. J.; Coulibaly, F.; Proft, T.; Baker, E. N. Crystal structure of Spy0129, a *Stectoccocus pyogenes* class B sortase involved in pilus assembly. *PLoS ONE*. **2011**, *6*(1): e15969.

39. Dramsi, S.; Caliot, E.; Bonne, I.; Guadagnini, S.; Prévost, M. C.; Kojadinovic, M.; Lalioui, L.; Poyart, C.; Trieu-Cout, P. Assembly and role of pili in group B streptococci. *Mol Microbiol*. **2006**, *60*(6): 1401-1413.

40. Hendrickx, A. P. A.; Budzik, J. A.; Oh, S. Y.; Schneewind, O. Architects at the bacterial surface — sortases and the assembly of pili with isopeptide bonds. *Nat Rev Microbiol*. **2011**, *9*(3):166-76.

41. Marraffini, L. A.; Schneewing, O. Targeting proteins to the cell wall of sporulating *Bacillus anthracis*. *Mol Mircobiol*. **2006**, *62*(5):1402-1417.

42. Swaminthan, A.; Mandlik, A.; Swierczynski, A.; Gaspar, A.; Das, A.; Ton-That, H. Housekeeping sortase facilitates the cell wall anchoring of pilus polymers in *Corynebacterium diptheriae*. *Mol Microbiol*. **2007**, *66*(4): 961-974.

43. Williamson, D. J.; Fascione, M. A.; Webb, M. E.; Turnbull, W. B. Efficient N-terminal labeling of proteins by use of sortase. *Angew Chem Int Ed*. **2012**, *51*: 9377-9380.

44. Leung, M. K. M.; Hagemeyer, C. E.; Johnson, A. P. R.; Gonzales, C.; Kamphuis, M. M. J.; Ardipadja, K.; Such, G. K.; Peter, K.; Caruso, F. Bio-click chemistry: enzymatic functionalization of PEGylated capsules for targeting applications. *Angew Chem Int Ed*. **2012**, *51*: 1-5.

45. Zhang, J.; Wang, M.; Tang, Rui.; Liu, Y.; Lei, C.; Huang, Y.; Nie, Z.; Yao, S. Transpeptidation-mediated assembly of tripartite split GFP for label-free assay of sortase activity. *Anal Chem.* **2018**, *90*(5): 3245-3252.

46. Pritz, S.; Wolf, Y.; Kraetke, O.; Klose, J.; Bienert, M.; Beyermann, M. Synthesis of biologically active peptide nucleic acid-peptide conjugates by sortase-mediated ligation. *J Org Chem*. **2007**, *72*: 3909-3912.

47. Chen, I.; Dorr, B. M.; Liu, D. R. A general strategy for the evolution of bond-forming enzymes using yeast display. *PNAS*. **2011**, *108*(28): 11399-11404.

48. Hirakawa, H.; Ishikawa, S.; Nagamune, T. Design of Ca^{2+}-independent *Staphylococcus aureus* sortase A mutants. *Biotechnol Bioeng*. **2012**, *109*: 2955–2961.

49. Yamamura, Y.; Hirakawa, H.; Yamaguchi, S.; Nagamune, T. Enhancement of sortase A-mediated protein ligation by inducing a β-hairpin structure around the ligation site. *Chem Commun*. **2011**, *47*: 4742-4744.

50. Liu, F.; Luo, E. Y.; Flora, D. B.; Mezo, A. R. irreversible sortase A-mediated ligation driven by diketopiperazine formation. *J Org Chem*. **2014**, *79*: 487-492.

51. Row, R. D.; Roark, T. J.; Philip, M. C.; Perkins, L. L.; Antos, J. M. Enhancing the efficiency of sortase-mediated ligations through nickel-peptide complex formation. *Chem Commun*. **2015**, *51*: 12548-12551

52. Witte, M. D.; Theile, C.; Wu, T.; Guimaraes, C. P.; Blom, A. E. M.; Ploegh, H. L. production of annaturally linked chimeric proteins using a combination of sortase-catalyzed transpeptidation and click chemistry. *Nat Protoc*. **2013**, *8*(9): 1808-1819.

53. Zahnd, C.; Wyler, E.; Schwenk, J. M.; Steiner, D.; Lawrence, M. C.; McKern, N. M.; Pecorari, F.; Ward, C. W.; Joos, T. O.; Plückthun, A. A designed ankyrin repeat protein evolved to picomolar affinity to HER2. *J Mol Biol*. **2007**, *369*: 1015-1028.

54. Eigenbrot, C.; Ultsch, M.; Dubnovitsky, A.; Abrahmsén, L.; Härd, T. Structural basis for high-affinity HER2 receptor binding by an engineered protein. *PNAS*. **2010**, *107*(34): 15039-15044.

55. Plückthun, A. Designed ankyrin repeat proteins (DARPins): binding proteins for research, diagnostics, and therapy. *Annu Rev Pharmacol Toxicol*. **2015**, *55*: 489-511.

56. Ståhl, S.; Gräslund, T.; Karslträm, A. E.; Frejd, F. Y.; Nygren, P-A.; Löfblom, J. Affibody molecules in biotechnological and medical applications. *Trends Biotechnol*. **2017**, *35*(8): 691-712.

57. Kükenshöner, T.; Schmit, N. E.; Bouda, E.; Sha, F.; Pojer, F.; Koide, A.; Seeliger, M.; Koide, S.; Hantchel, O. Selective targeting of SH2 domain-phosphotyrosine

interactions of the Src family tyrosine kinases with monobodies. *J Mol Biol*. **2017**, *429*: 1364-1380.

58. Schlatter, D.; Brack, S.; Banner, D. W.; Batey, S.; Benz, J.; Bertschinger, J.; Huber, W.; Joseph, C.; Rufer, A. C.; van der Klooster, A.; Weber, M.; Grabulovski, D.; Hennig, M. Generation, characterization and structural data of chymase binding proteins based on the human Fyn kinase SH3 domain. *mAbs*. **2012**, *4*(4): 497-508.

59. Koide, A.; Bailey, C. W.; Huang, X.; Koide, S. The fibronectin type III domain as a scaffold for novel binding proteins. *J Mol Biol*. **1998**, *284*: 1141-1151.

60. Grabulovski, D.; Kaspar, M.; Neri, D. A novel, non-immunogenic Fyn SH#-derived binding protein with tumor vascular targeting protperties. *J Biol Chem*. **2007**, *282*(5): 3196-3204.

61. Fraga, H.; Faria, T. Q.; Pinto, F.; Almeida, A.; Briot, R. M. M.; Damas, A. M. FH8 – a small EF-hand protein from *Fasciola hepatica*. *FEBS J*. **2010**, *277*(24): 5072-5085.

62. Vasquez-Lombardi, R.; Phan, T. G.; Zimmermann, C.; Lowe, D.; Jermutus, L.; Christ, D. Challenges and opportunities for non-antibody scaffold drugs. *Drug Discov Today*. **2015**, *20*(10): 1271-1283.

63. Westerlund, K.; Honarvar, H.; Tolmachev, V.; Karlström, A. E. Design, preparation, and characterization of PNA-based hydribization probes for affibody-molecule-mediated pretargeting. *Bioconjugate Chem*. **2015**, *26*: 1724-1736.

64. Popp, M. W.; Dougan, S. K.; Chuang, T. Y.; Spooner, E.; Ploegh, H. L. Sortase-catalyzed transformations that improve the properties of cytokines. *PNAS*. **2011**, *108*(8): 3169-3174.

65. Nag, A.; Mitra, G.; Ghosh, P. C. A colorimetric assay for estimation of polyethylene glycol and polyethylene glycolated proteins using ammonium ferrothiocyanate. *Anal Biochem*. **1996**, *237*: 224-231.

66. Debets, M. F.; van Hest, J. C. M.; Rutjes, F. P. J. T. Bioorthogonal labeling of biomolecules: new functional handles and ligation methods. *Org Biomol Chem.* **2013**, *11*: 6439-6455.

67. Patterson, D. M.; Nazarova, L. A.; Prescher, J. A. Finding the right (biorthogonal) chemistry. *ACS Chem Biol*. **2014**, *9*L 592-605.

68. Baskin, J. M.; Prescher, J. A.; Laughlin, S. T.; Agard, N. J.; Chang, P. V.; Miller, I. A.; Lo, A.; Codelli, J. A.; Bertozzi, C. R. Copper-free click chemistry for dynamic *in vivo* imaging. *PNAS*. **2007**, *104*(43): 16793-16797.

7. Appendix

7.1 Appendix I: Representative Mass Spectra from the Synthesis of GGK^{DBCO}

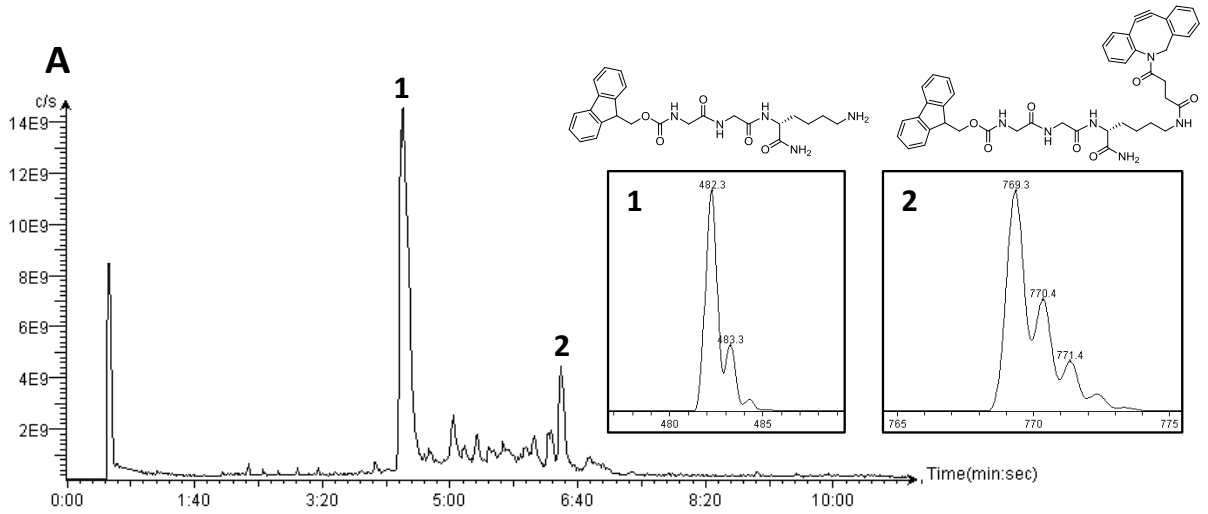

ESI-MS TIC from the ligation step, 25min after initiation. Peak **1** corresponds to unreacted Fmoc-GGK, the base peptide for the nucleophile (expected: 482.2 Da, observed: 482.3 Da). Peak **2** represents the conjugated product (expected: 769.3 Da, observed: 769.3 Da).

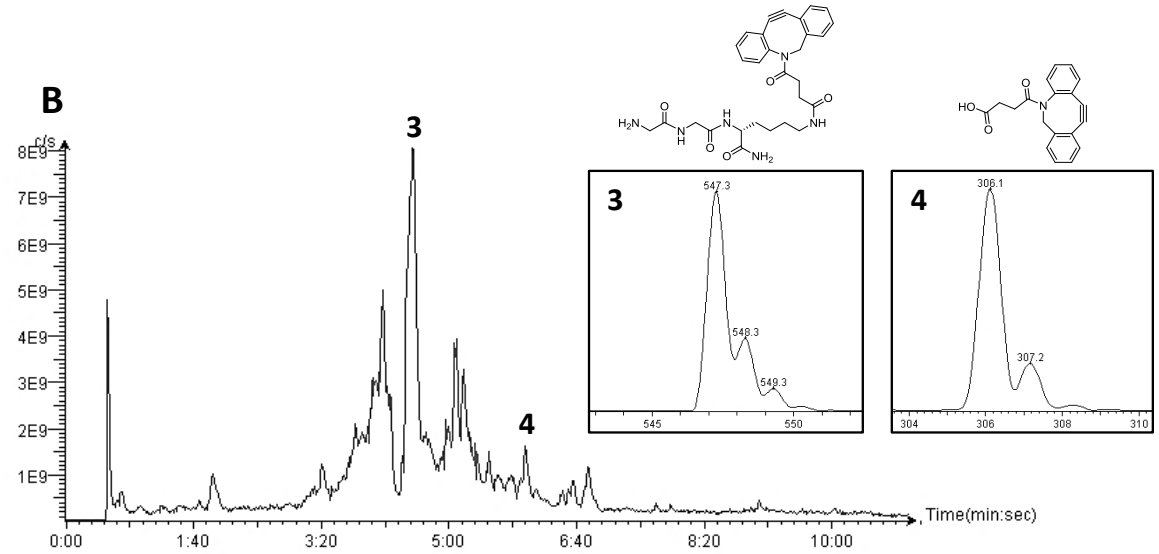

ESI-MS TIC from the deprotection step, 25min after adding piperidine. Peak **3** corresponds to deprotected GGK^{DBCO} (expected: 547.3 Da, observed: 547.3 Da). Peak **4** represents hydrolyzed DBCO (expected: 306.1 Da, observed: 306.1 Da).

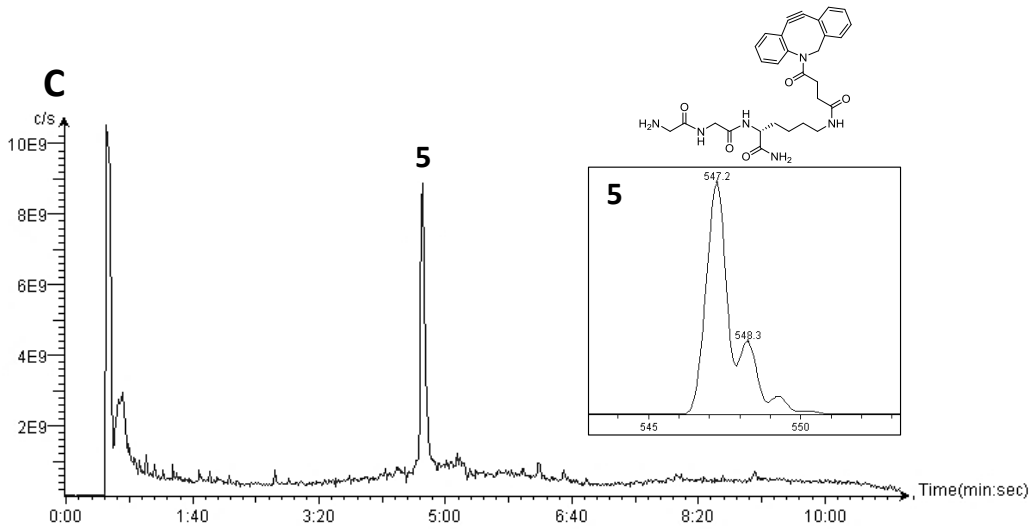

ESI-MS TIC of the purified GGK^{DBCO} stock at reaction concentration (50µM). Peak **5** corresponds to the final product, GGK^{DBCO} (expected: 547.3 Da, observed: 547.2 Da).

7.2 Appendix II: Analytical RP-HPLC and ESI-MS Data for Peptide Nucleophiles

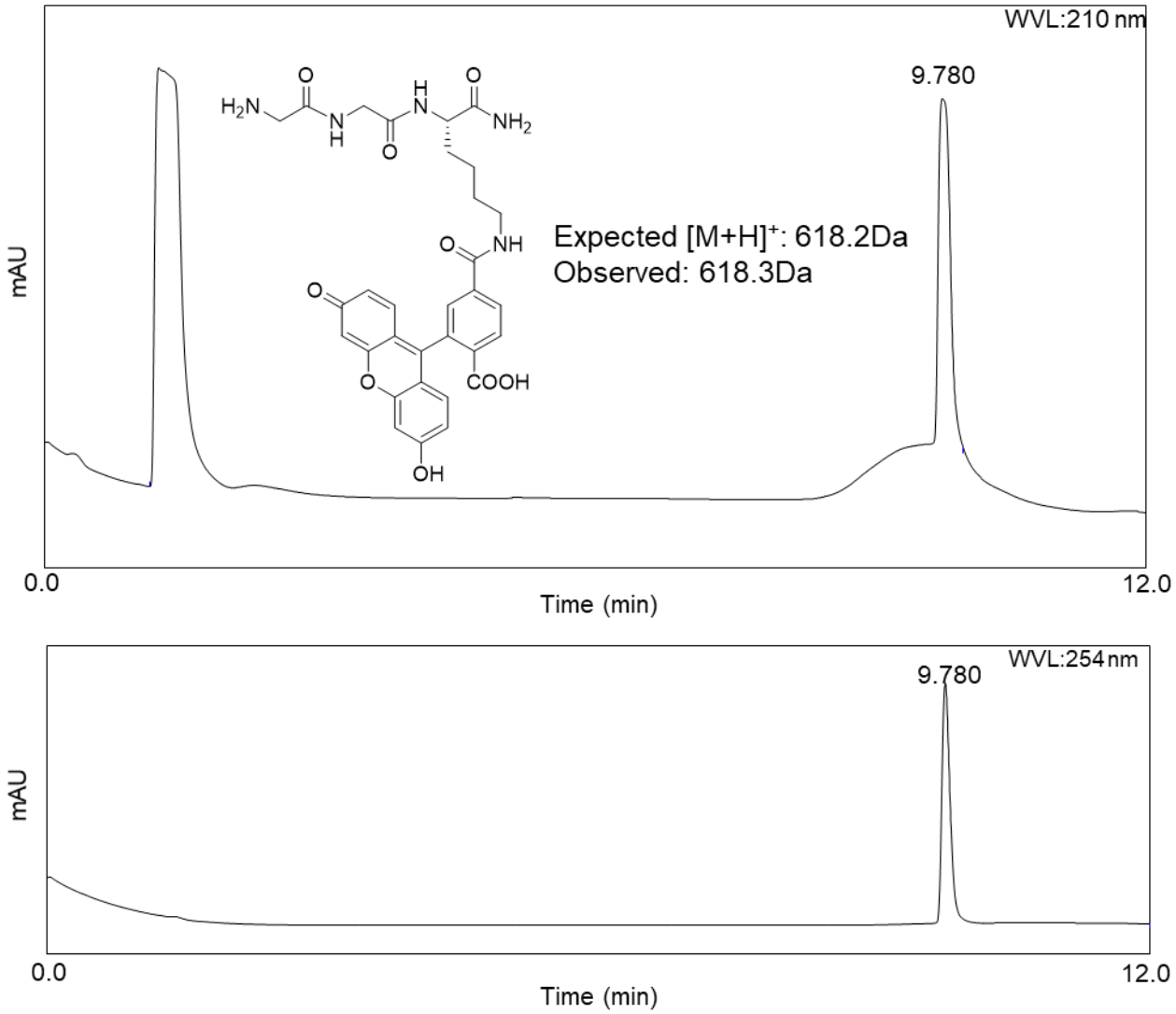

UV-Vis analysis of GGK(6-FAM) stock at 50µM. (Top) Absorbance at 210nm, with nucleophile structure and ESI-MS data reported. (Bottom) Absorbance at the λ_{max} of the nucleophile.

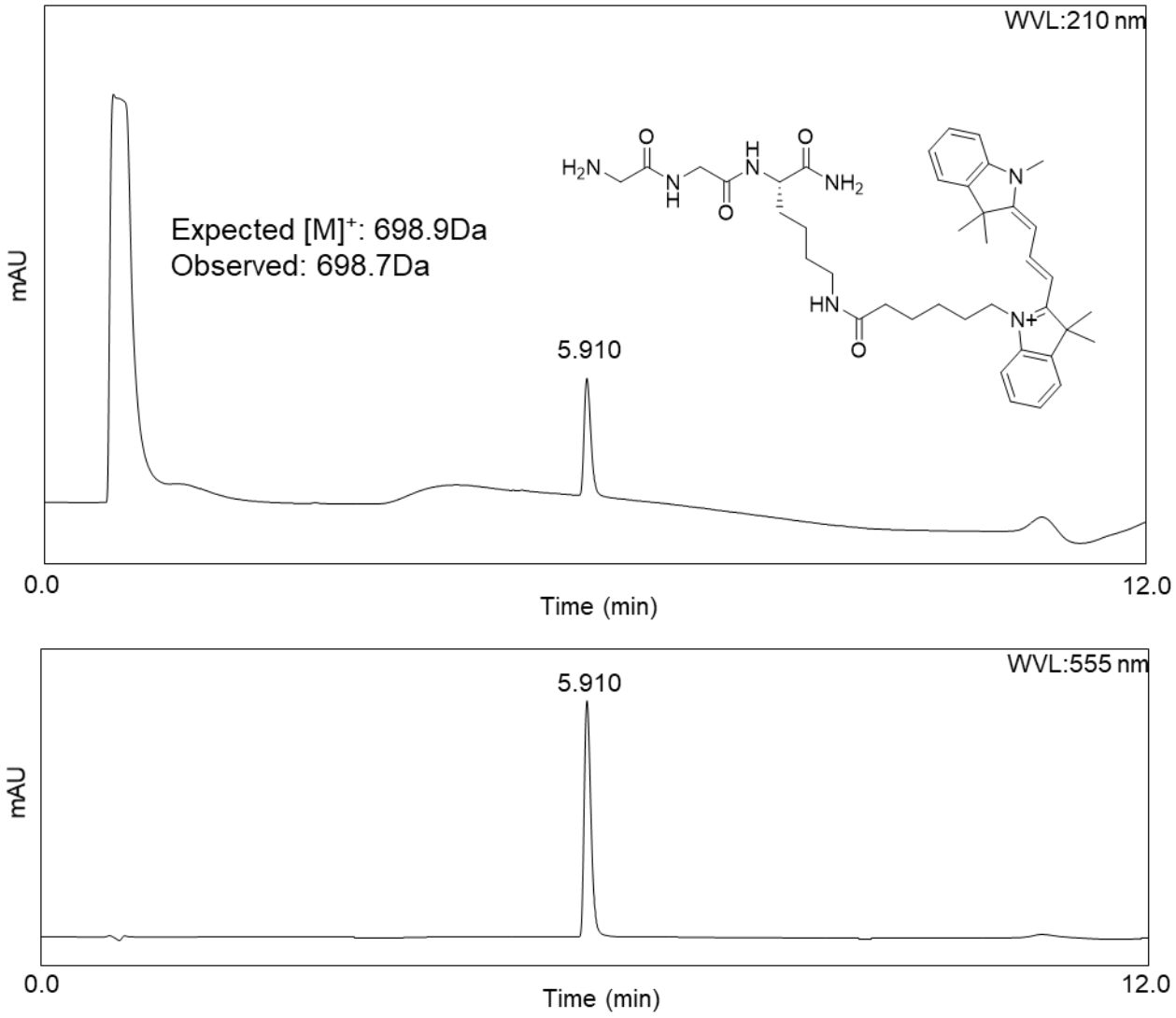

UV-Vis analysis of GGK(Cy3) stock at 50µM. (Top) Absorbance at 210nm, with nucleophile structure and ESI-MS data reported. (Bottom) Absorbance at the λ_{max} of the nucleophile.

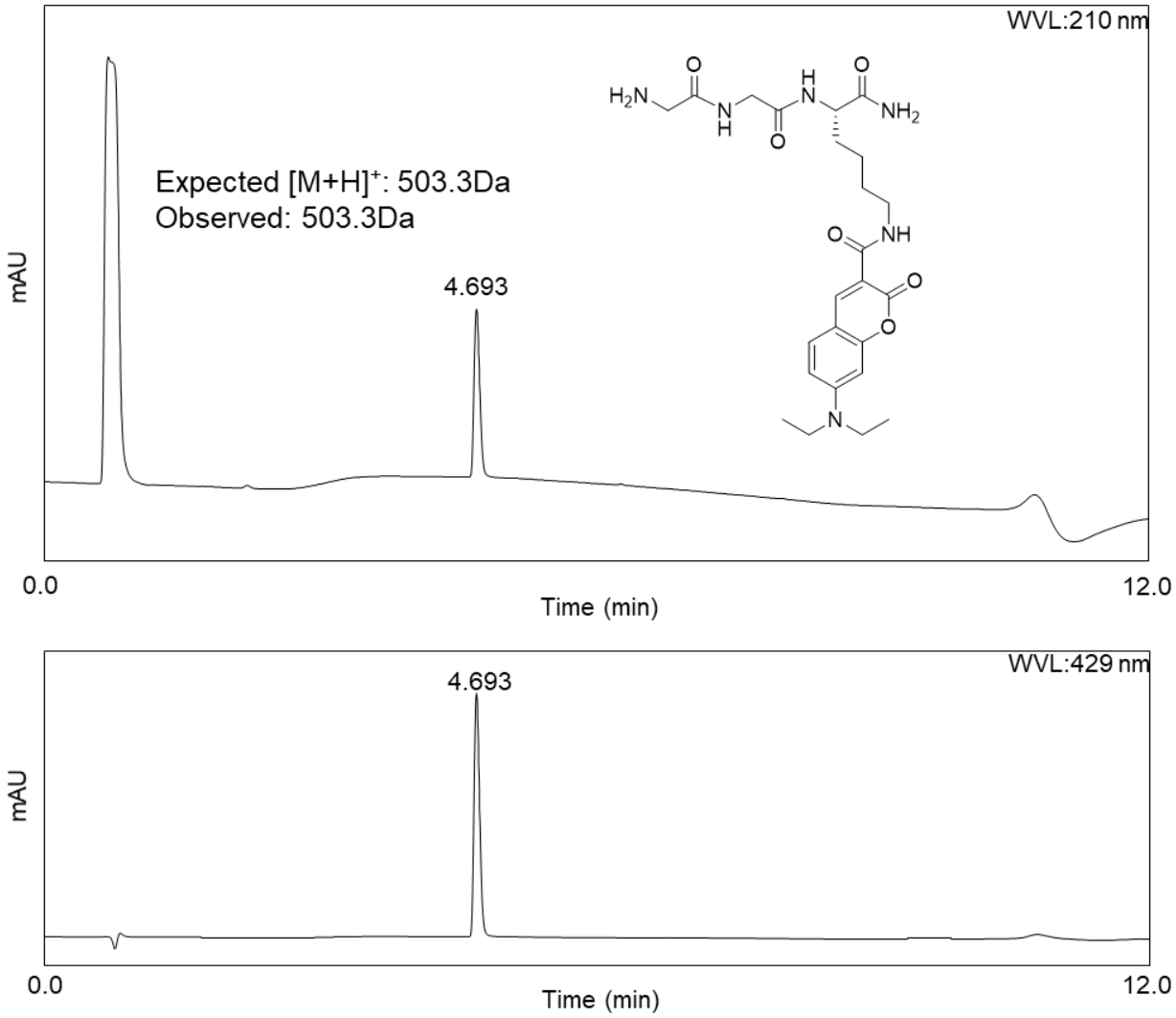

UV-Vis analysis of GGK(DEAC) stock at 50µM. (Top) Absorbance at 210nm, with nucleophile structure and ESI-MS data reported. (Bottom) Absorbance at the λ_{max} of the nucleophile.

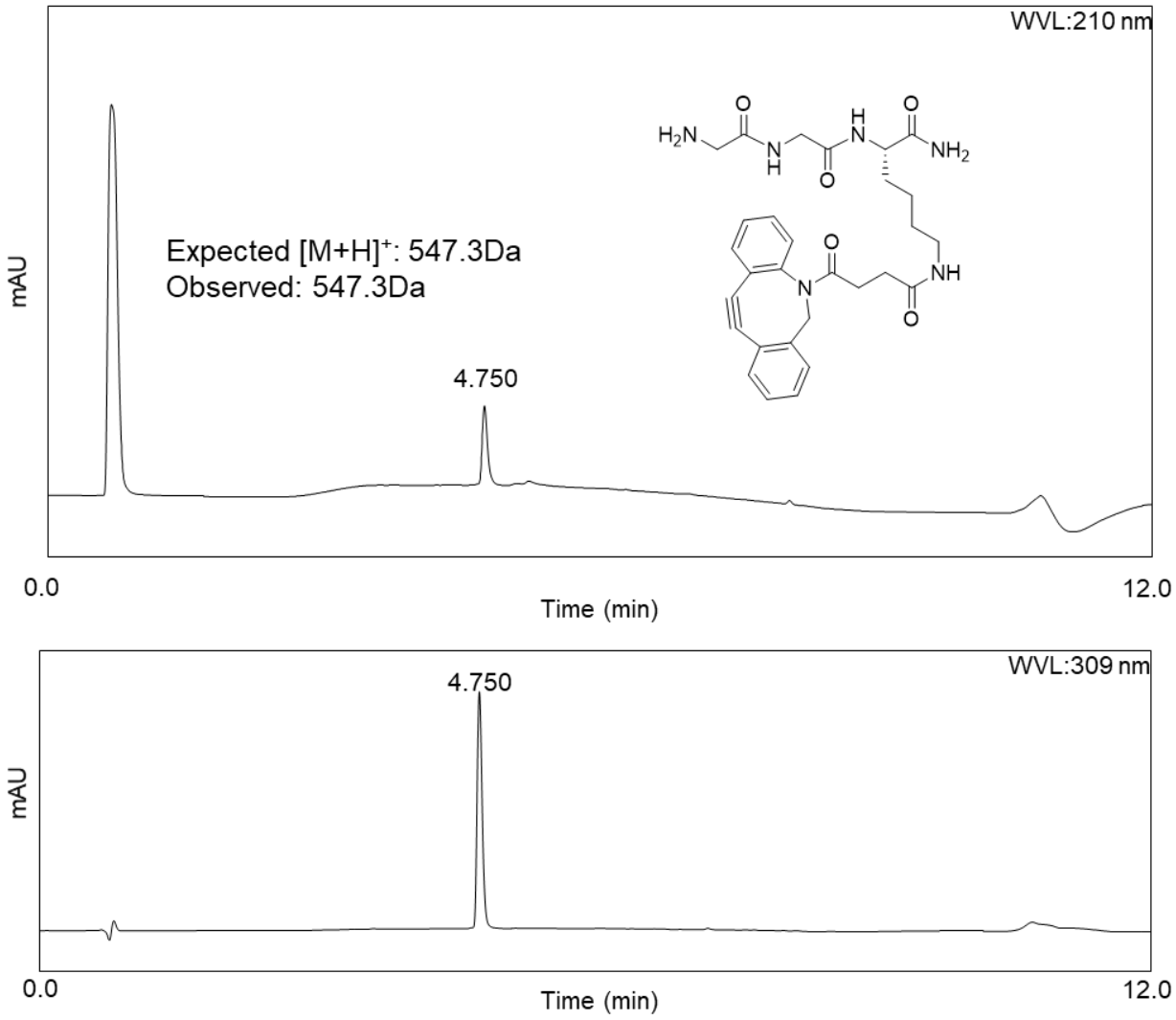

UV-Vis analysis of GGK(DBCO) stock at 50µM. (Top) Absorbance at 210nm, with nucleophile structure and ESI-MS data reported. (Bottom) Absorbance at the λ_{max} of the nucleophile.

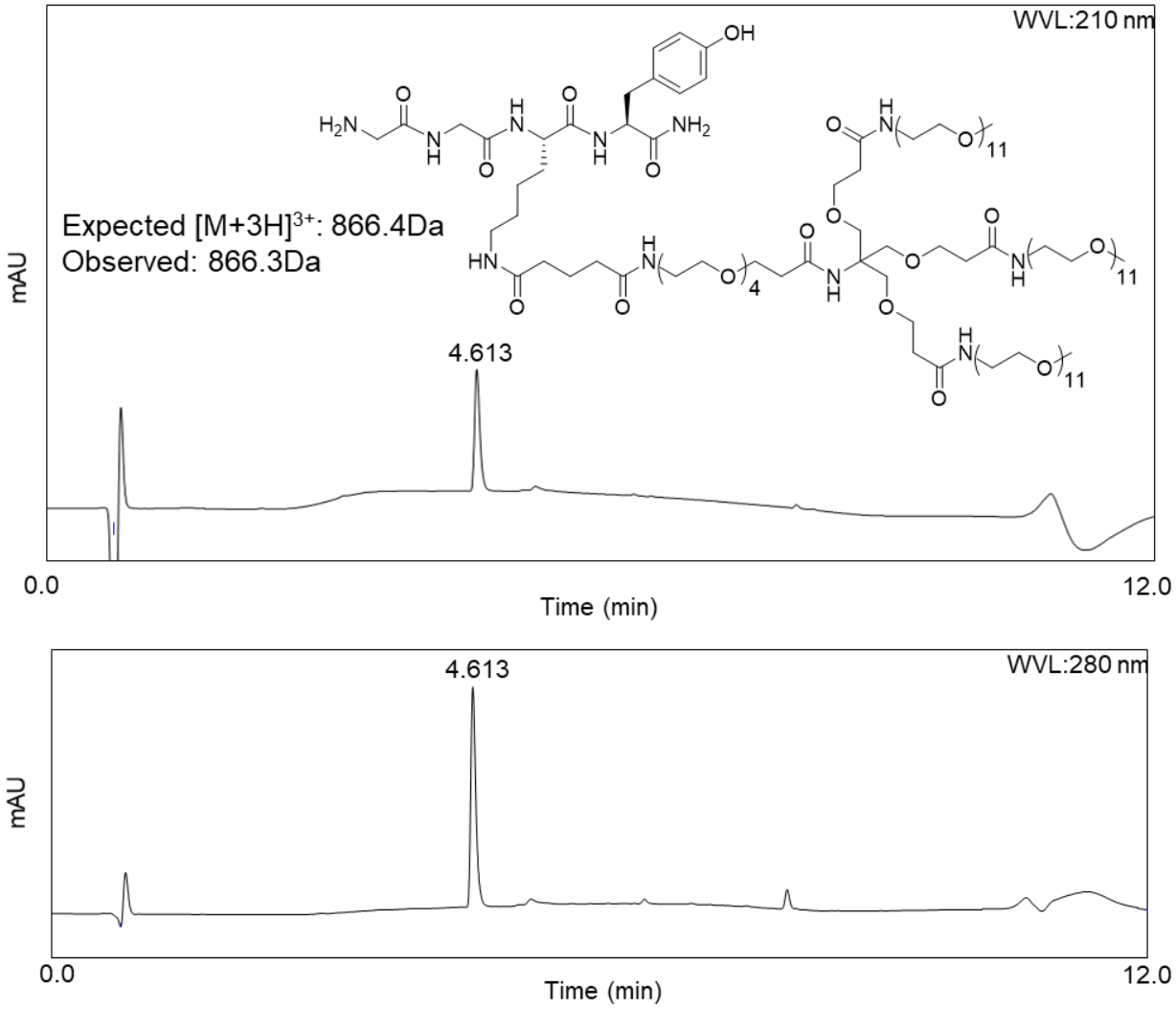

UV-Vis analysis of GGK(dPEG2000) stock at 50μM. (Top) Absorbance at 210nm, with nucleophile structure and ESI-MS data reported. (Bottom) Absorbance at the λ_{max} of the nucleophile.

7.3 Appendix III: Analytical ESI-MS and SDS-PAGE Data for Protein Substrates

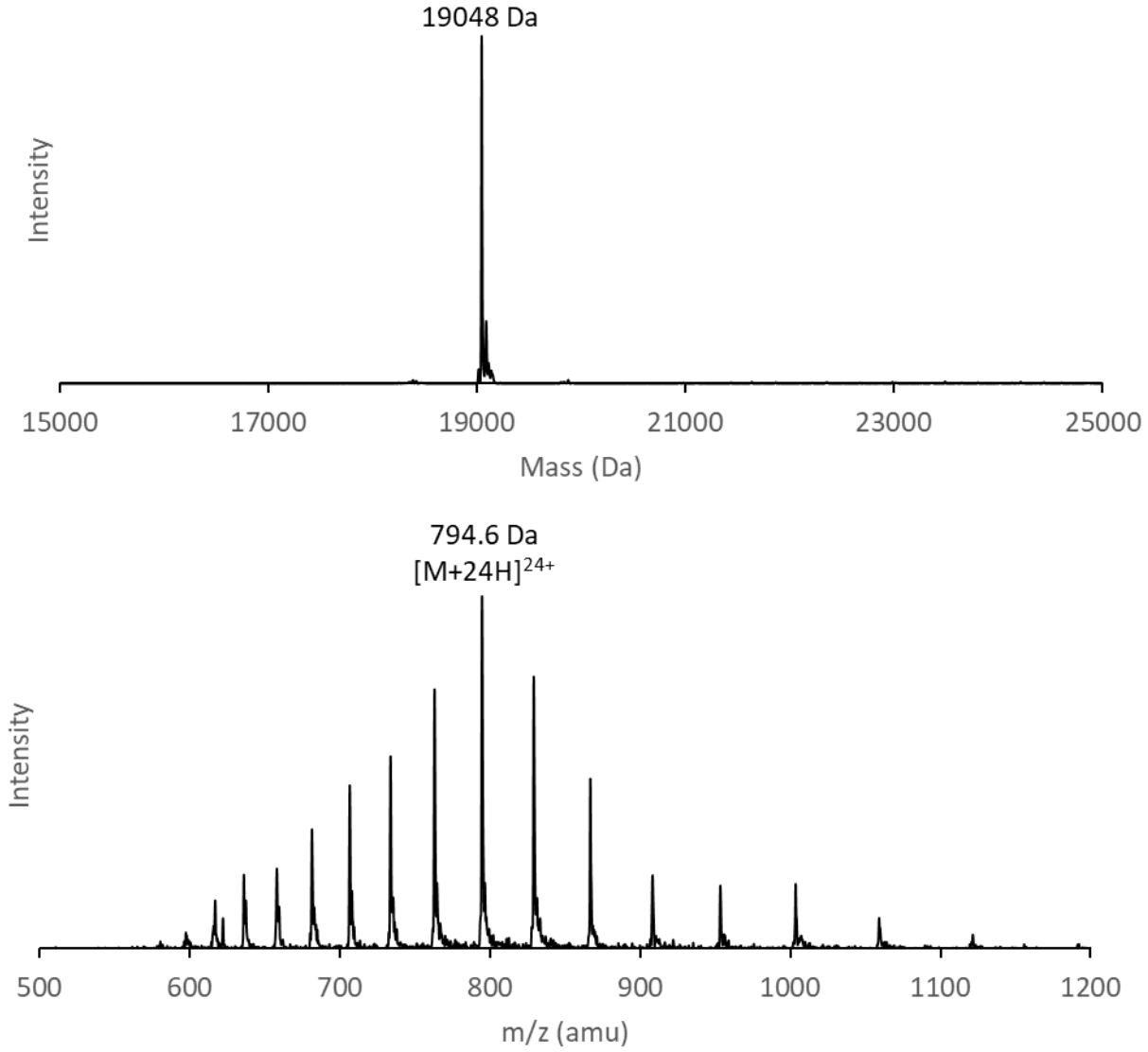

ESI-MS analysis of $SrtA_{Staph}$ stock. (Top) Reconstructed mass graph. (Bottom) Charge ladder, with main peak labeled with mass and charge state. Expected mass: [M] = 19048 Da, $[M+24H]^{24+}$ = 794.7 Da.

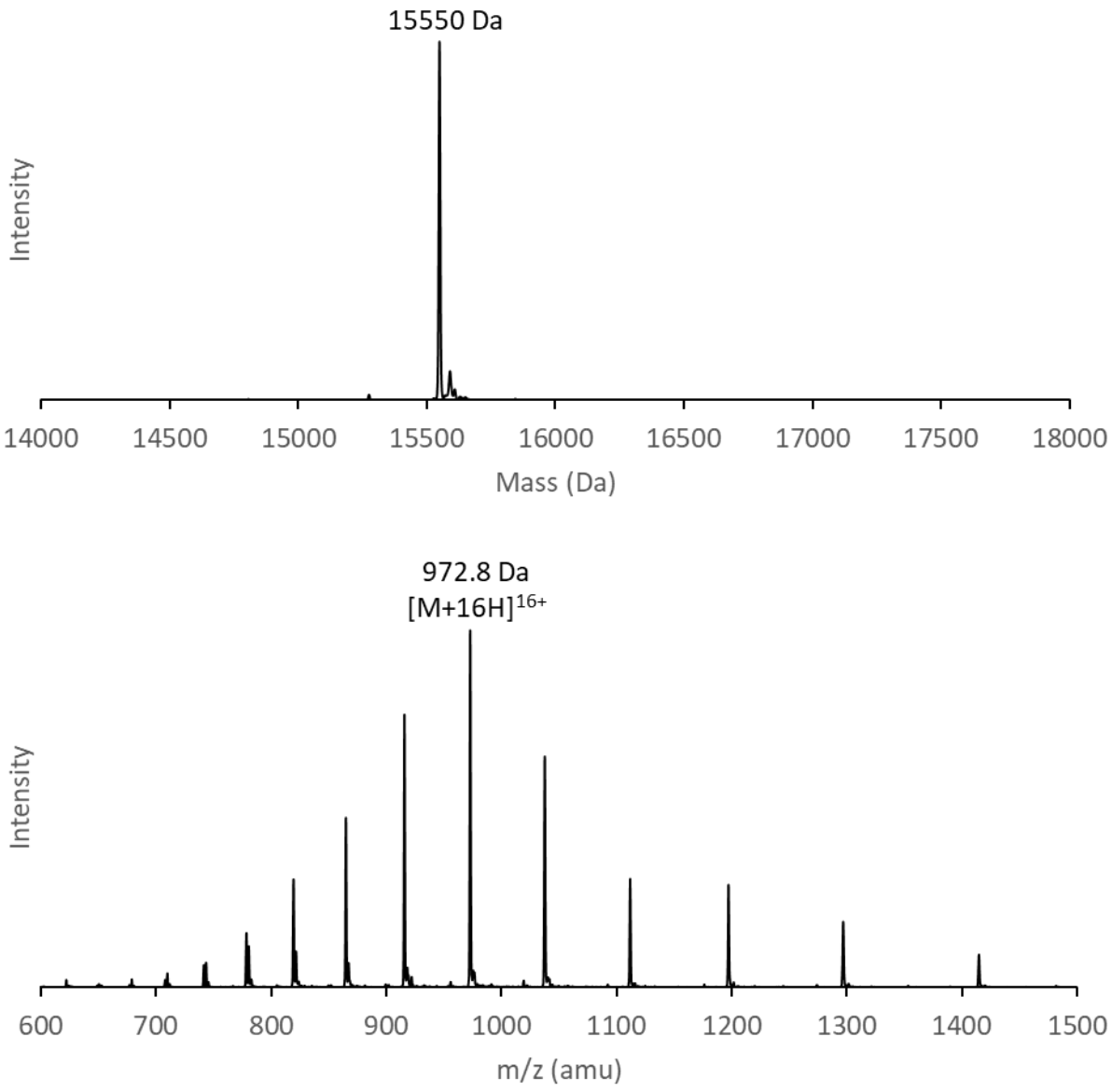

ESI-MS analysis of sDARP stock. (Top) Reconstructed mass graph. (Bottom) Charge ladder, with main peak labeled with mass and charge state. Expected mass: [M] = 15550 Da, $[M+16H]^{16+}$ = 972.9 Da.

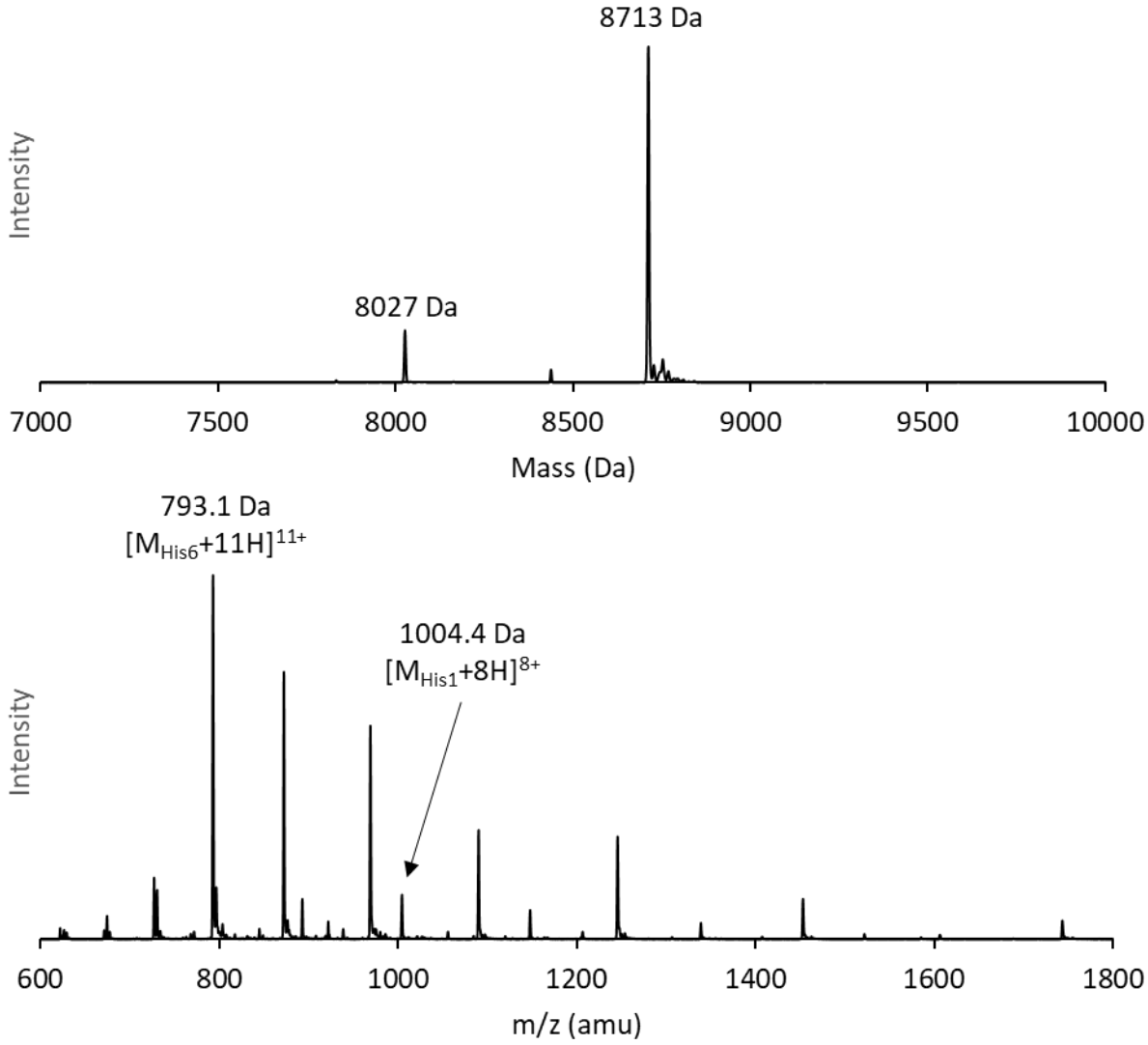

ESI-MS analysis of sAff stock. (Top) Reconstructed mass graph. (Bottom) Charge ladder, with main peak labeled with mass and charge state. Expected mass: [M_{His6}] = 8714 Da, [M_{His1}] = 8028 Da, [M_{His6}+11H]$^{11+}$ = 793.2 Da, [M_{His1}+8H]$^{8+}$ = 1004.5 Da.

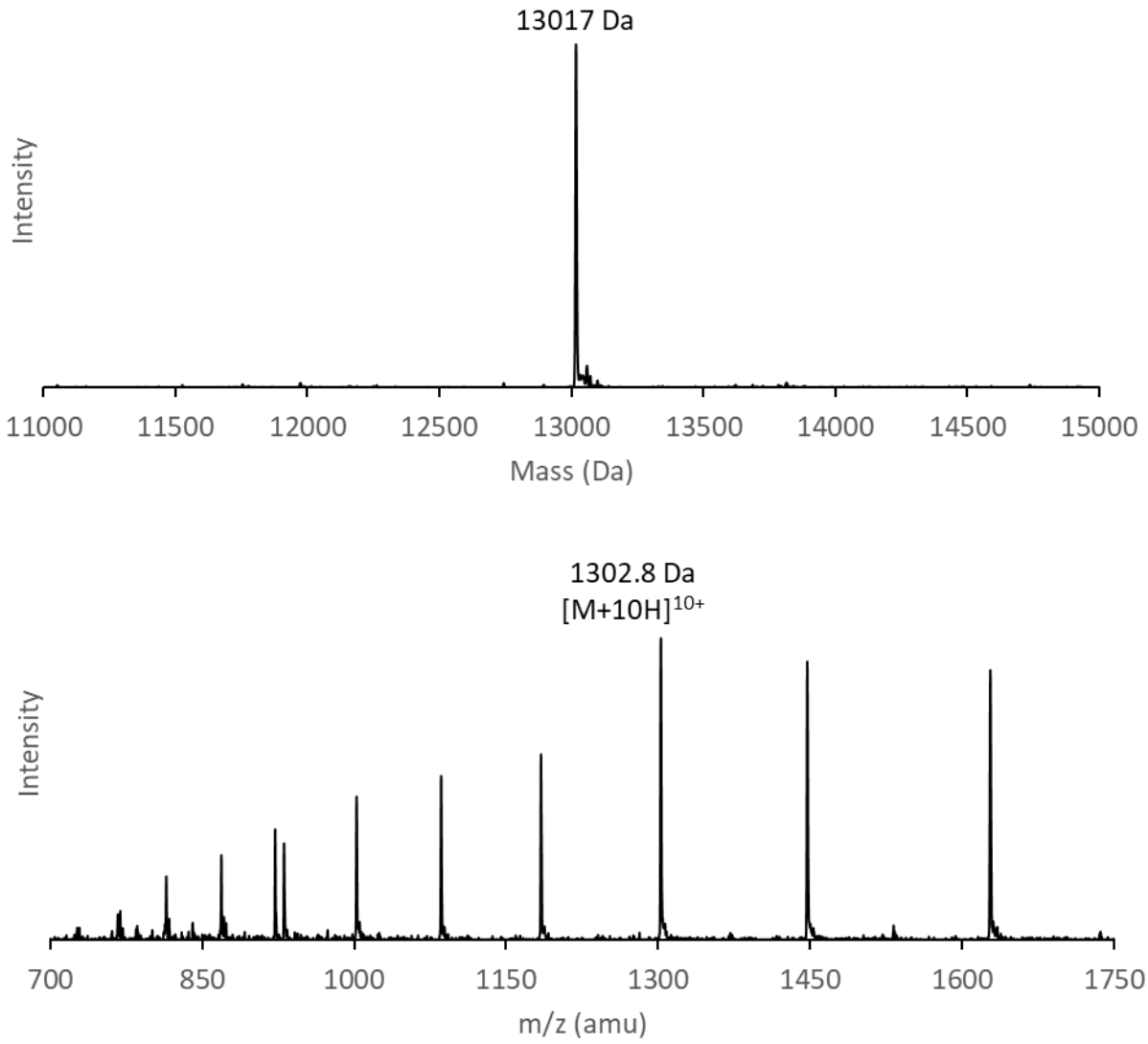

ESI-MS analysis of sMon stock. (Top) Reconstructed mass graph. (Bottom) Charge ladder, with main peak labeled with mass and charge state. Expected mass: [M] = 13018 Da, $[M+10H]^{10+}$ = 1302.8 Da.

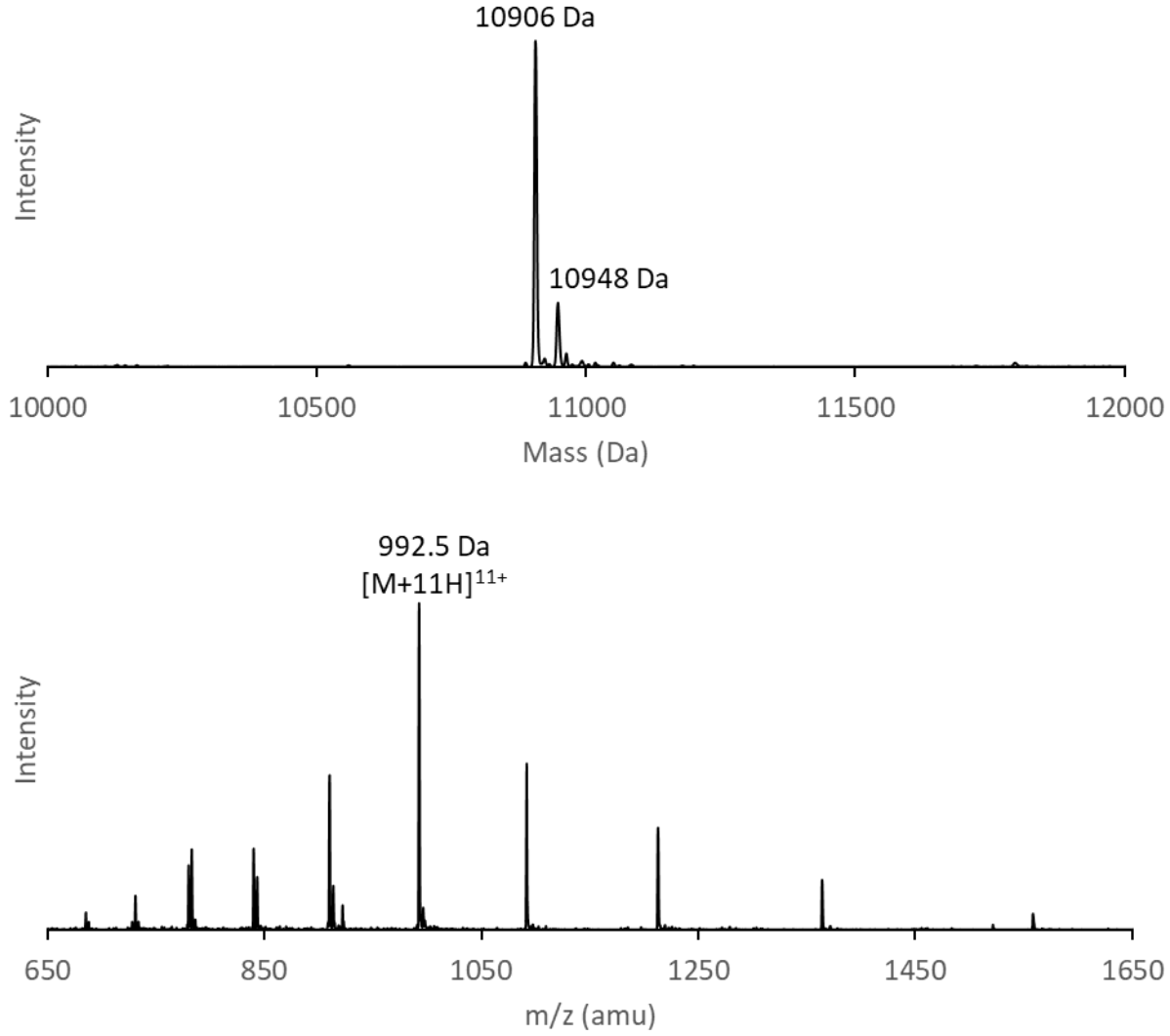

ESI-MS analysis of sFyn stock. (Top) Reconstructed mass graph. (Bottom) Charge ladder, with main peak labeled with mass and charge state. Expected mass: [M] = 10907 Da, [M+Ac] = 10949 Da, $[M+11H]^{11+}$ = 992.5 Da.

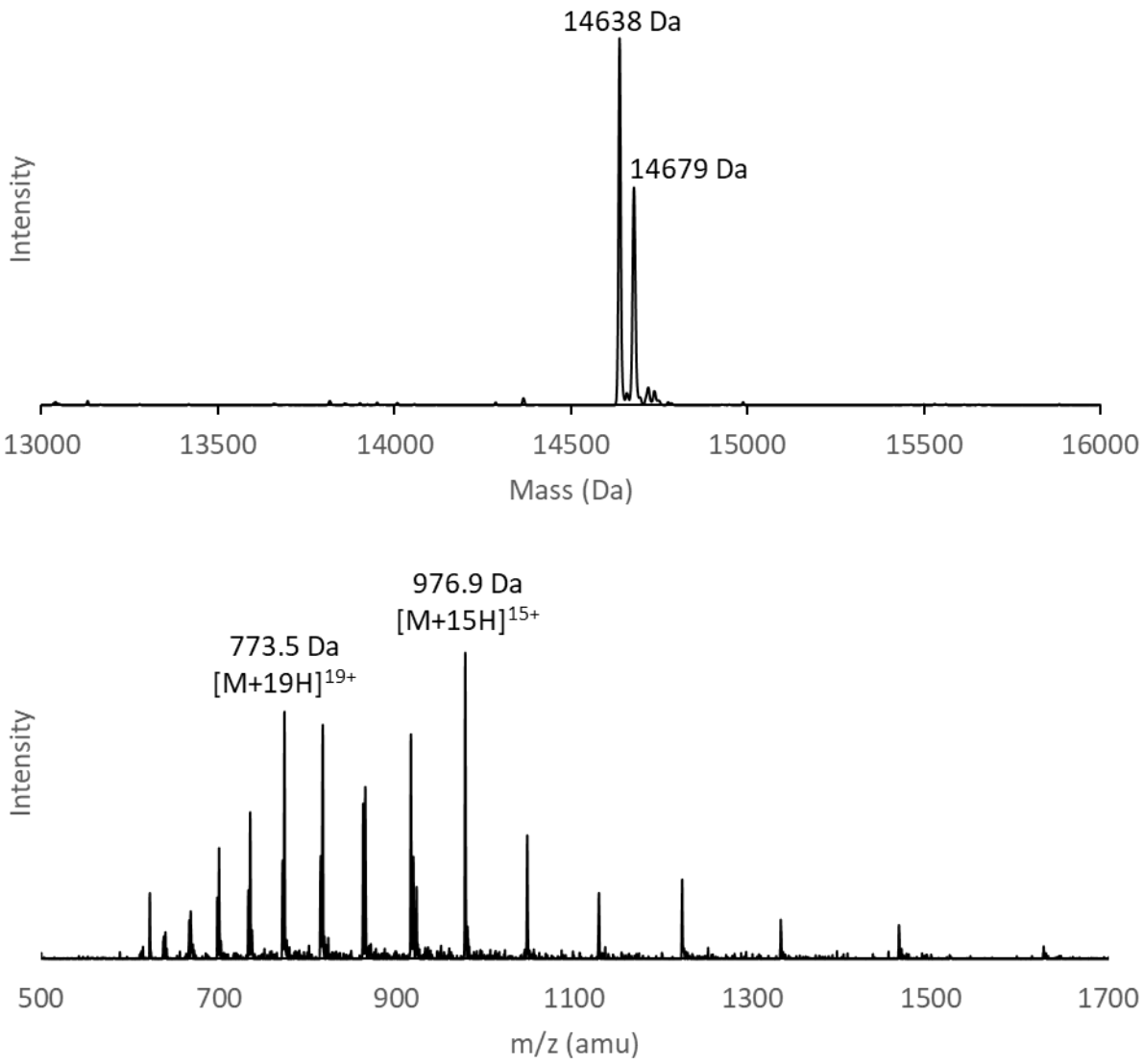

ESI-MS analysis of sFh8 stock. (Top) Reconstructed mass graph. (Bottom) Charge ladder, with main peak labeled with mass and charge state. Expected mass: [M] = 14636, [M+Ac] = 14678 Da, $[M+15H]^{15+}$ = 976.7 Da, $[M+Ac+19H]^{19+}$ = 773.5 Da.

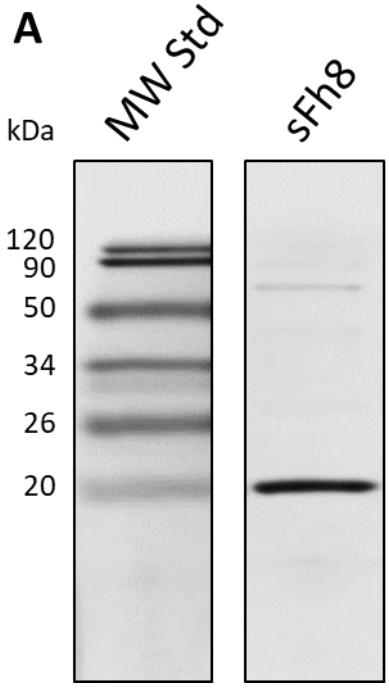

SDS-PAGE analysis of sFh8 (50µM), on a gel containing 15% acrylamide.

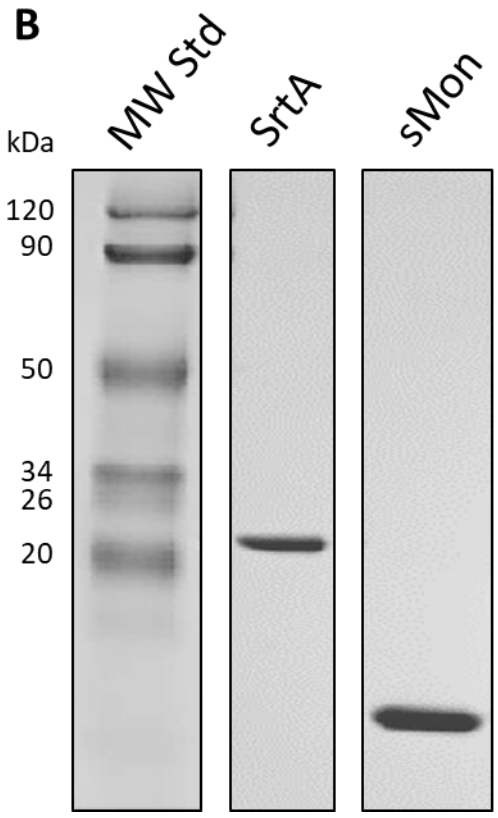

SDS-PAGE analysis of SrtA and sMon stocks (10µM and 50µM, respectively), on a gel containing an acrylamide gradient.

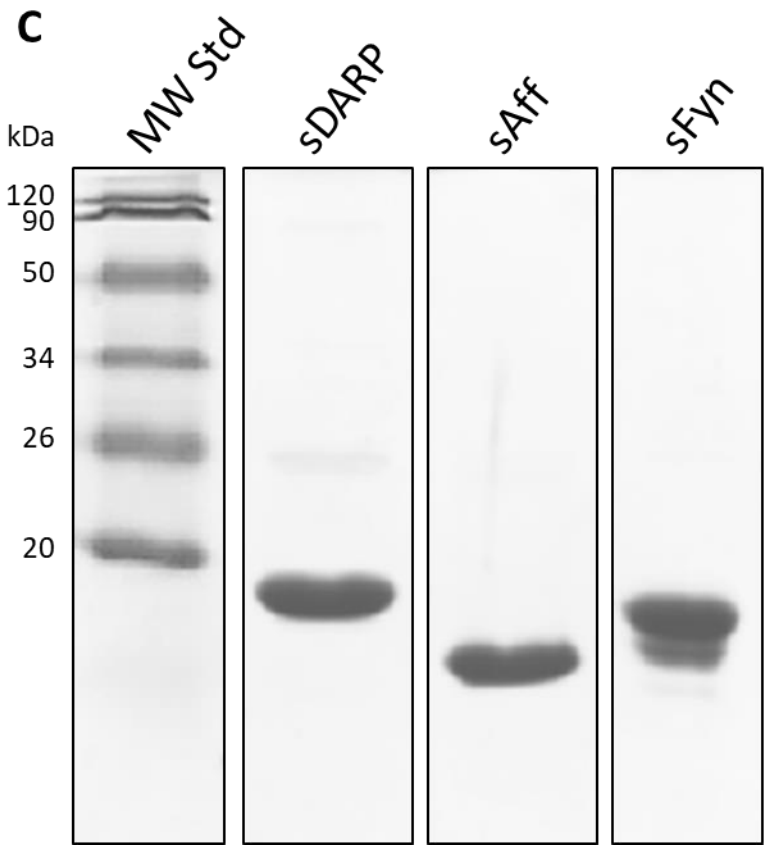

SDS-PAGE analysis of sDARP, sAff and sFyn stocks (50µM each), on a gel containing 15% acrylamide.